

Large Longitudinal Spin Alignment of Excited Projectiles in Intermediate Energy Inelastic Scattering

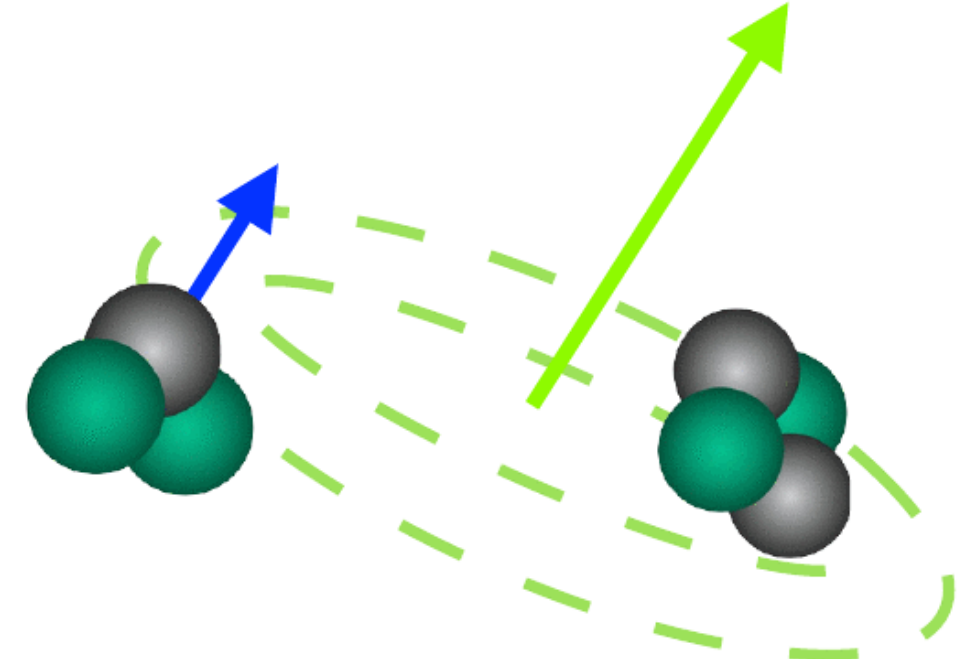
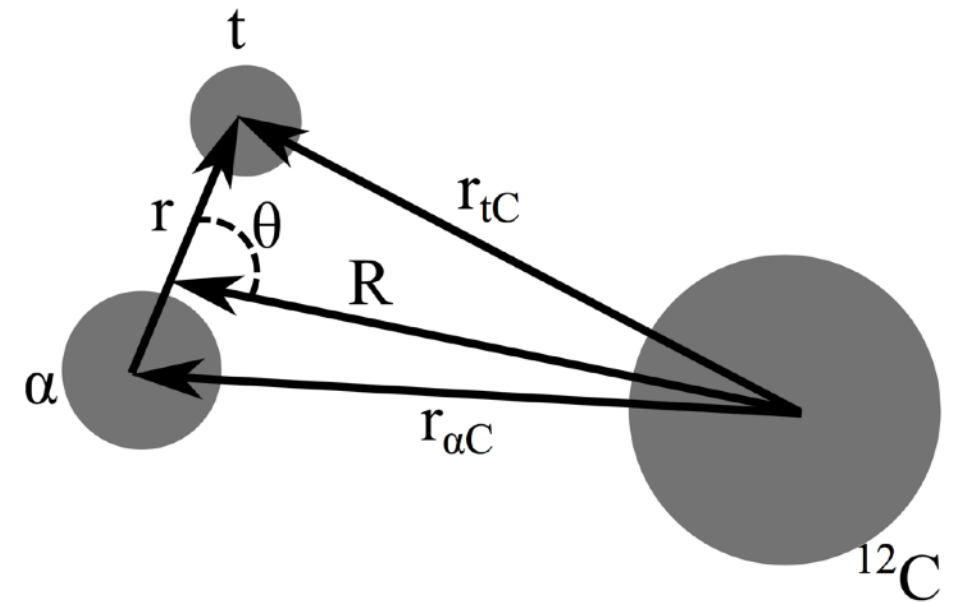
9/17/2017

LANL Nuclear Data Seminar

Dan Hoff
Ph.D Candidate
Washington University in St. Louis

Outline

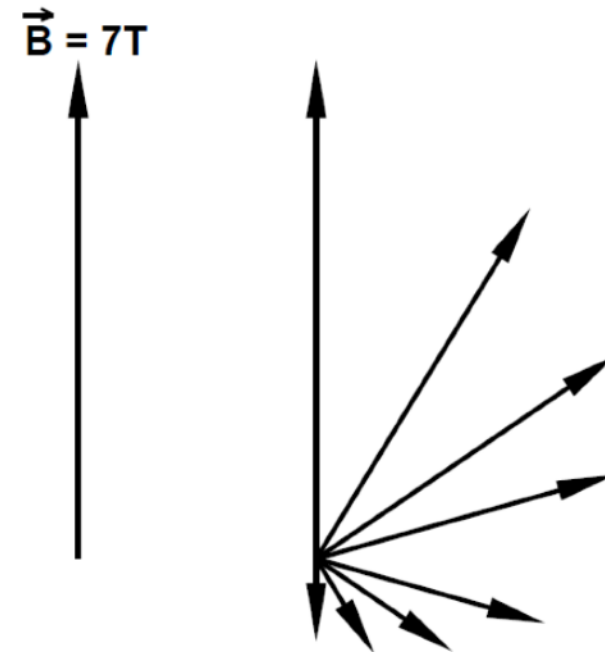
- Introduction
- Experiment
- Data analysis
- Alignment Mechanism and FRESCO calculations
- Conclusions



Introduction

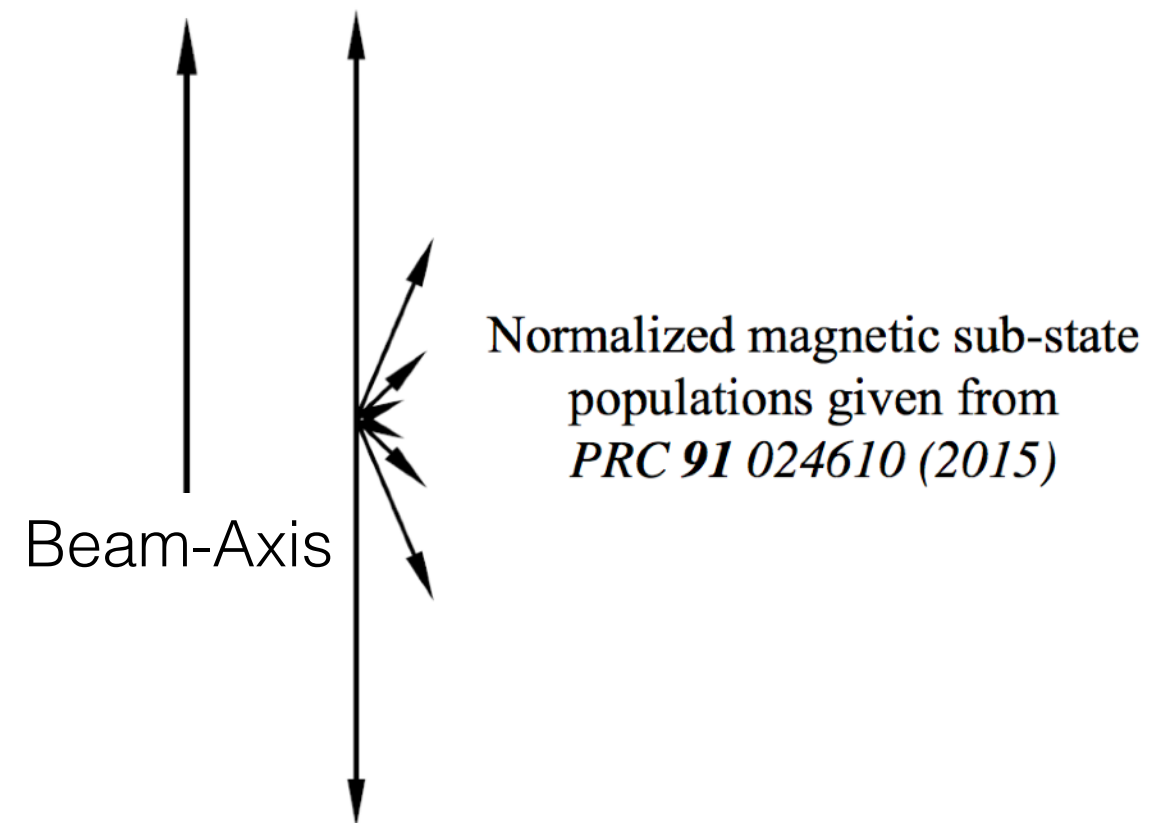
Polarization vs. Alignment

Polarization describes the spin of a particle pointing in mostly one direction
i.e. magnetic substates are lopsided.



Normalized magnetic sub-state populations for ${}^7\text{Li}^*(J^\pi = 7/2^-)$ in $B_0=7\text{T}$ at 20 mK

Alignment describes the spin of a particle pointing along an axis
i.e. magnetic substates are symmetric.



Introduction

- Alignment of nuclear states is useful for g-factor measurements.
- Alignment of molecular states allows for the production of highly polarized hydrogen targets.
- In compound, quasi-elastic, and deep inelastic reactions large alignment transverse to the beam-axis is common.
 - Can be used for fragment spin determination
 - Large alignments are also seen in relativistic Coulomb excitation.

Introduction

- Longitudinal alignment (parallel to the beam-axis) has been seen with projectile fragmentation.

- One can quantify the level of alignment with the scalar A ($1 = \text{max alignment}$, $-1 = \text{min alignment}$),

$$A = \sum_{m_f} \frac{3m_f - J(J+1)}{J(2J-1)} \rho_{m_f, m_f}^J$$

density matrix

- $A = 0.35$ is largest reported long alignment from projectile fragmentation.

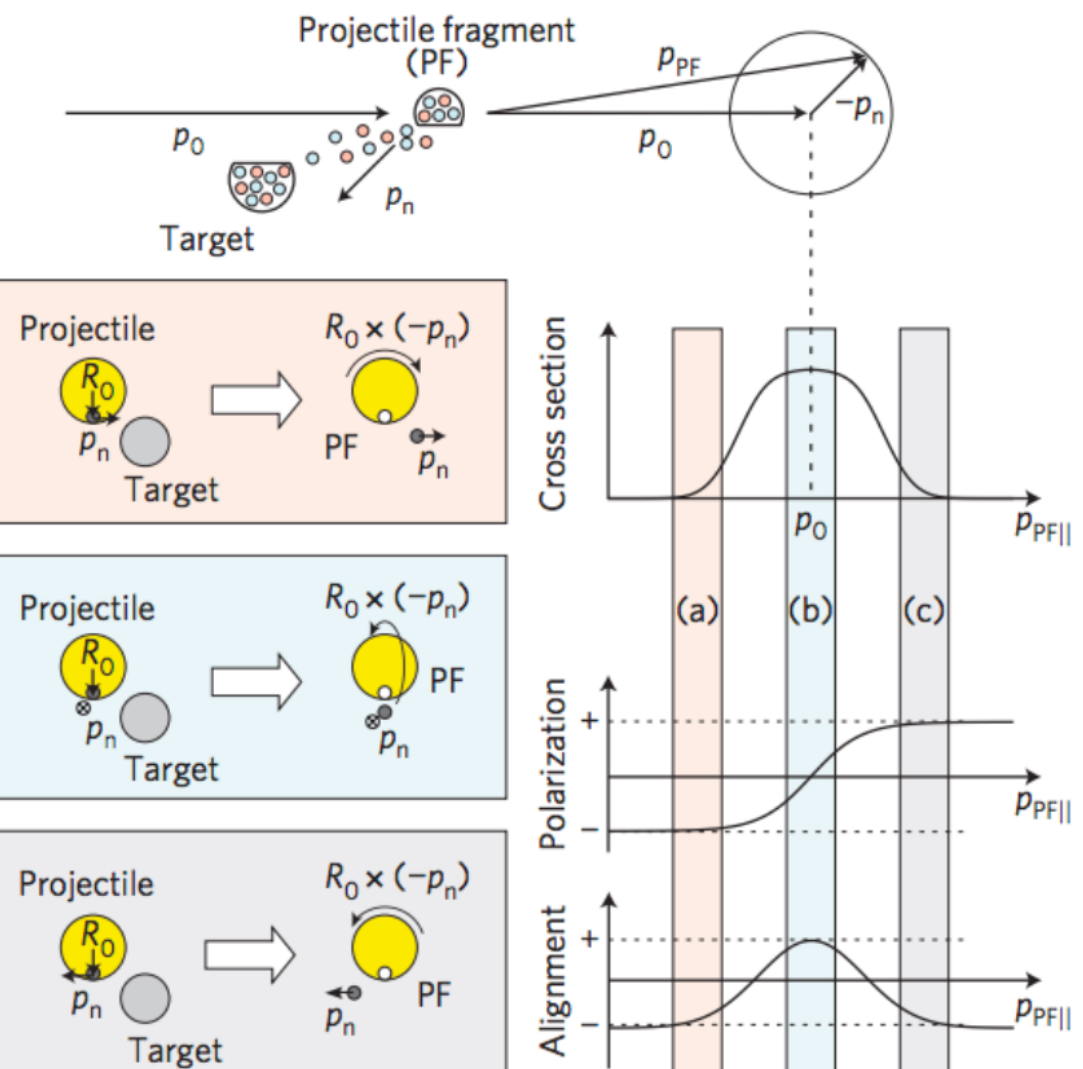
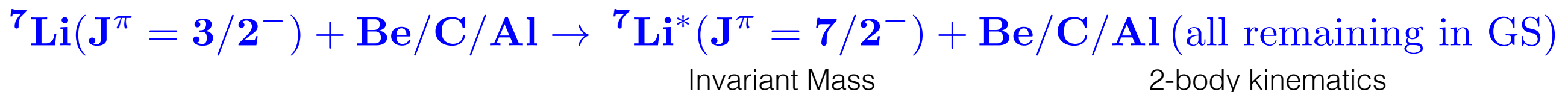


Figure 1. from *Nature Physics* 8, 918–922 (2012)

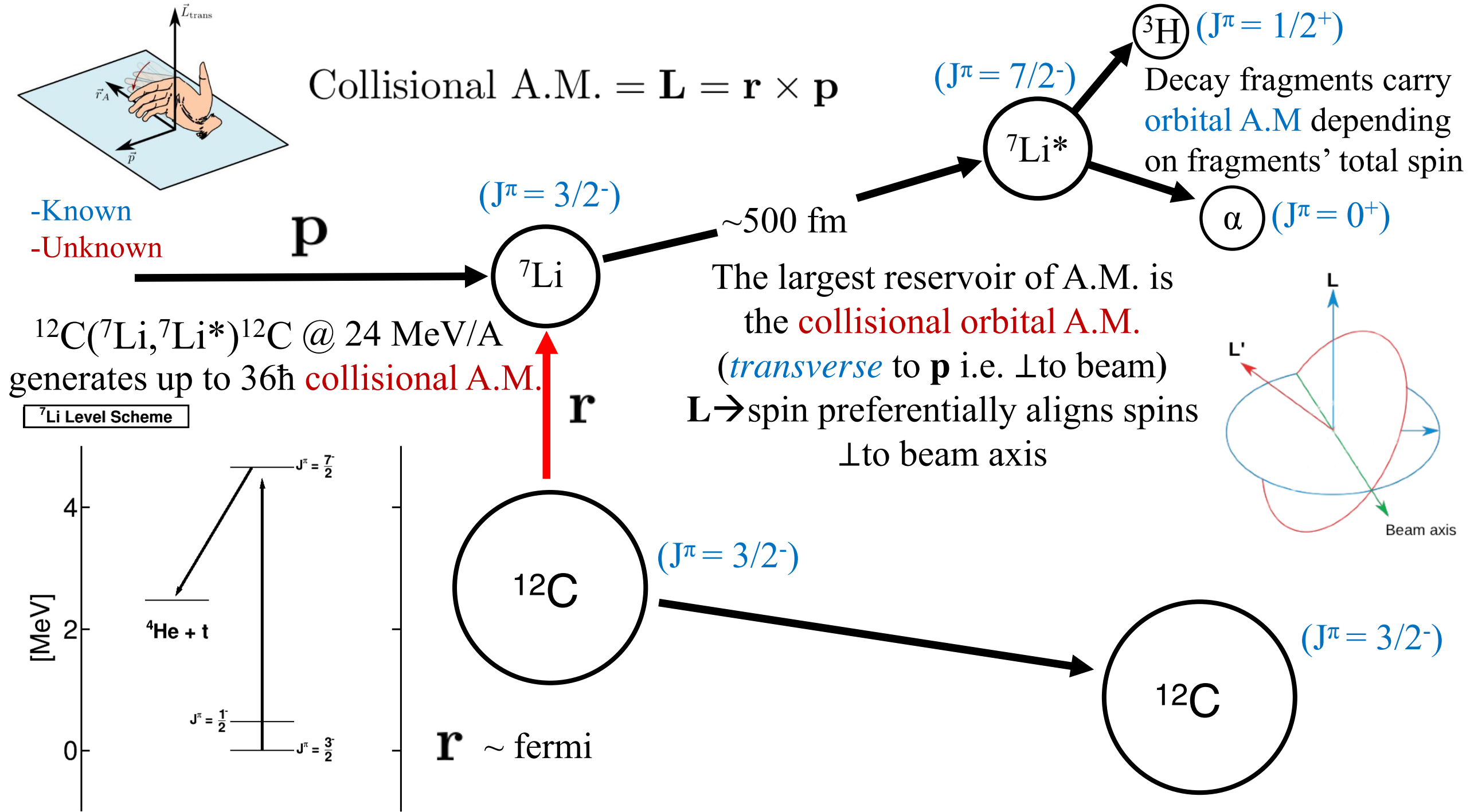
Experiment

- We studied three ${}^7\text{Li}$ reactions at 24 MeV/A at TAMU:



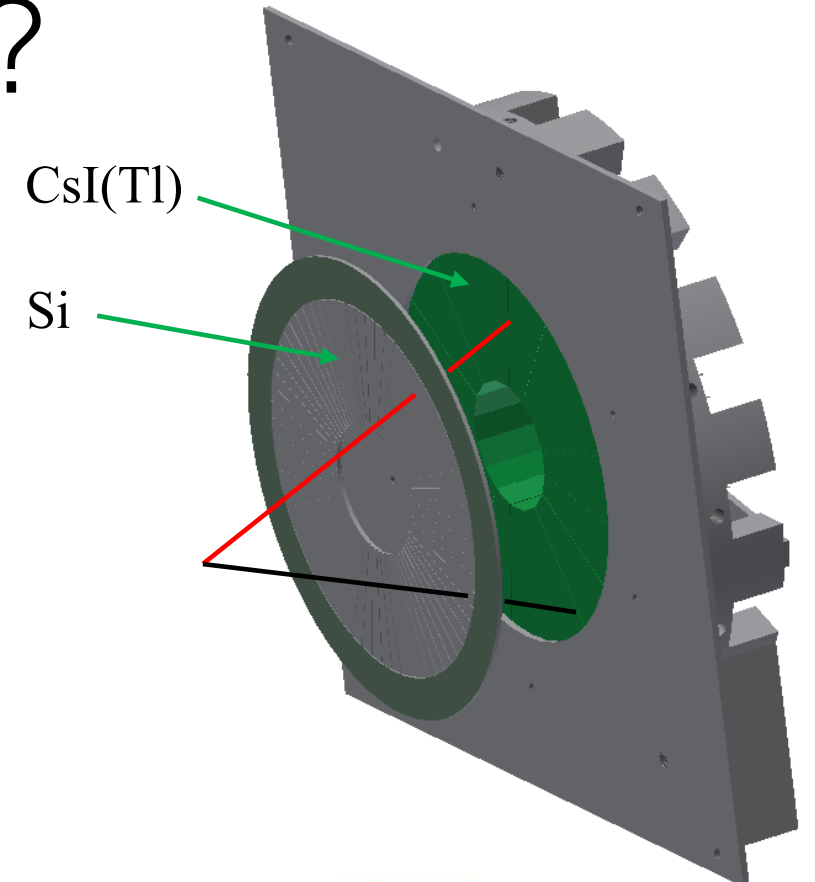
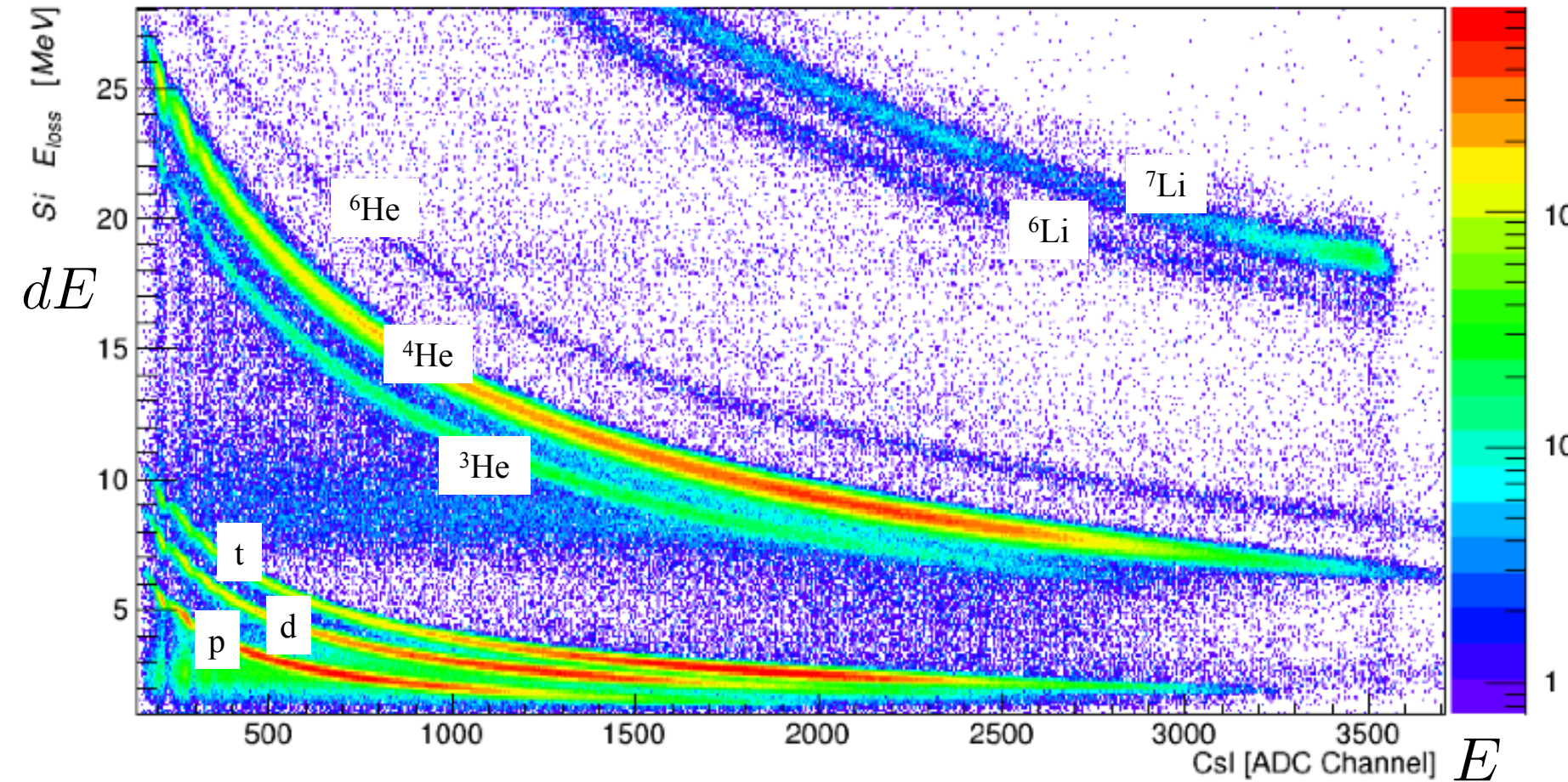
- We found a **large** spin alignment ($A = 0.49$) of ${}^7\text{Li}^*$ *longitudinal* to the beam axis for all three targets.
- Largest reported longitudinal alignment generated from nuclear reactions.
- This is not relativistic Coulomb excitation.
 - 24 MeV/A ${}^7\text{Li}$ is only slightly relativistic.
 - We only used low Z targets.

Experiment



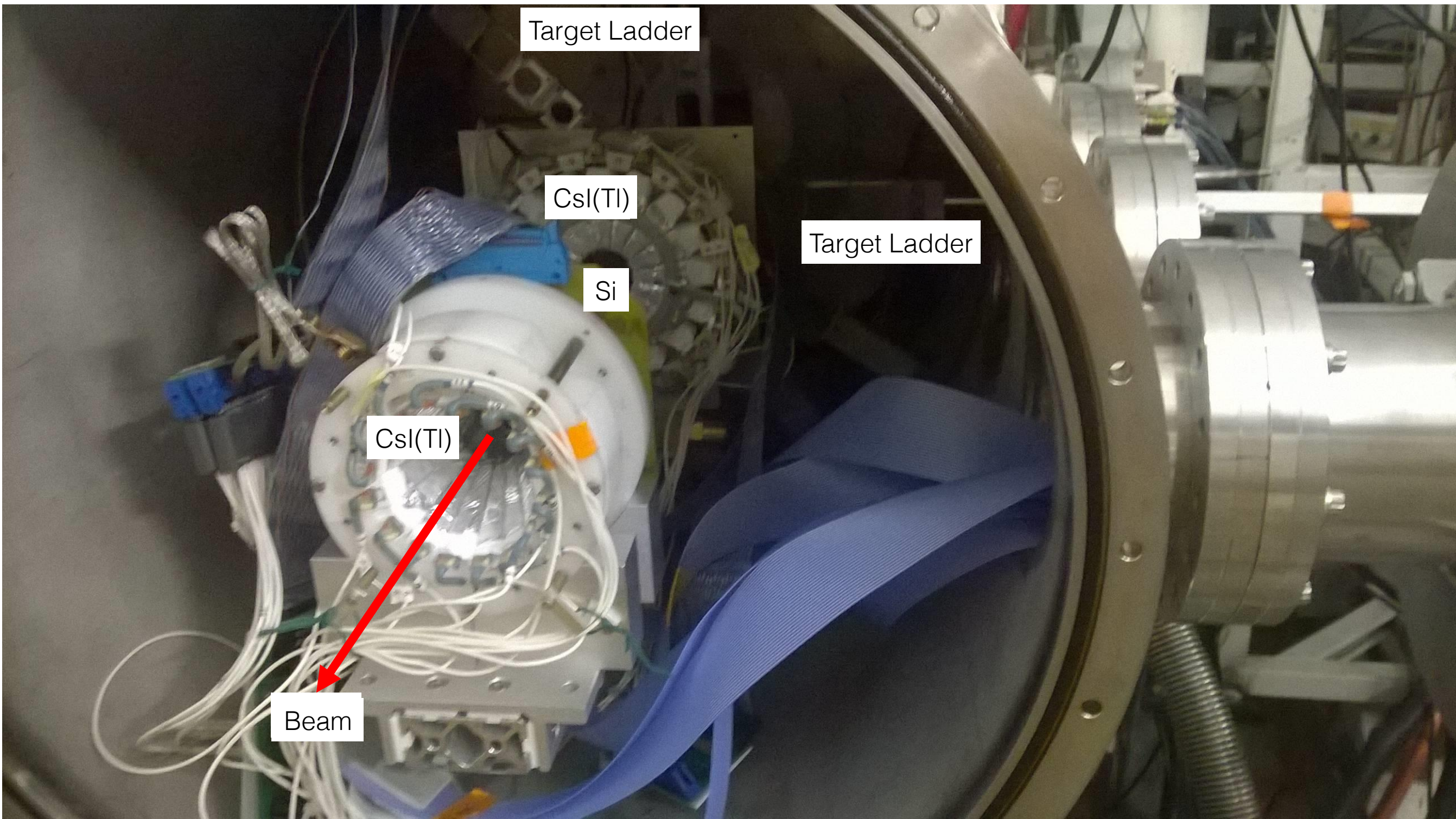
How do we measure projectile fragments ($\alpha+t$)?

- We used two annular Si-CsI(Tl) telescopes, one looking through the hole of the other →
- These allow us measure E , \vec{p} , and Particle ID of the projectile fragments.

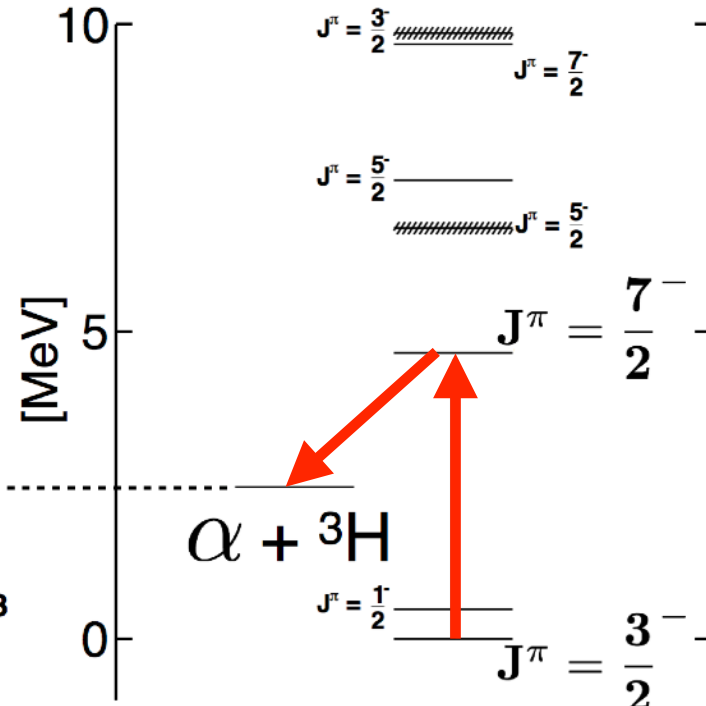
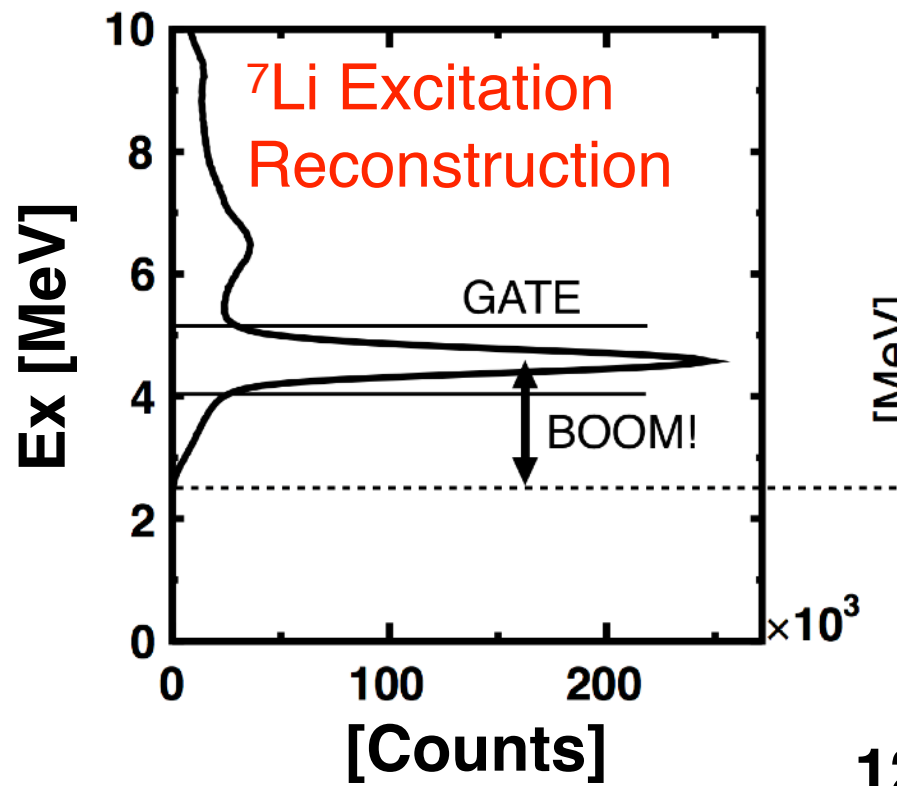


$$dE \propto \frac{Z^2 A}{E}$$

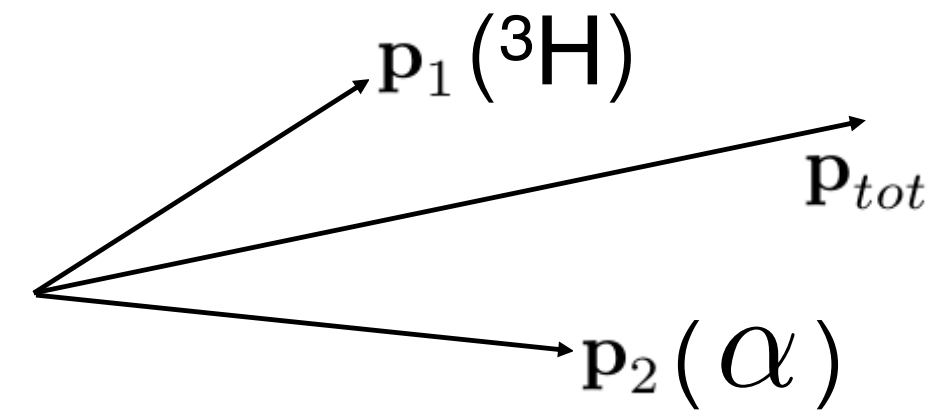
Setup at TAMU MARS line



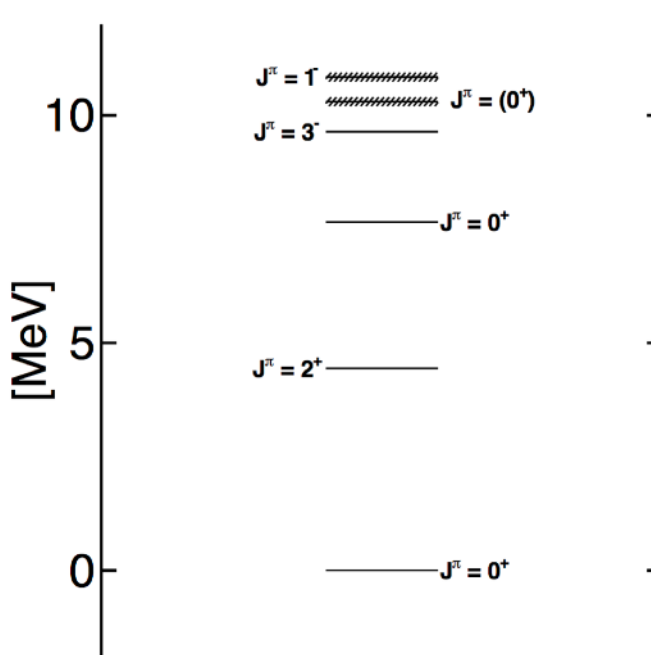
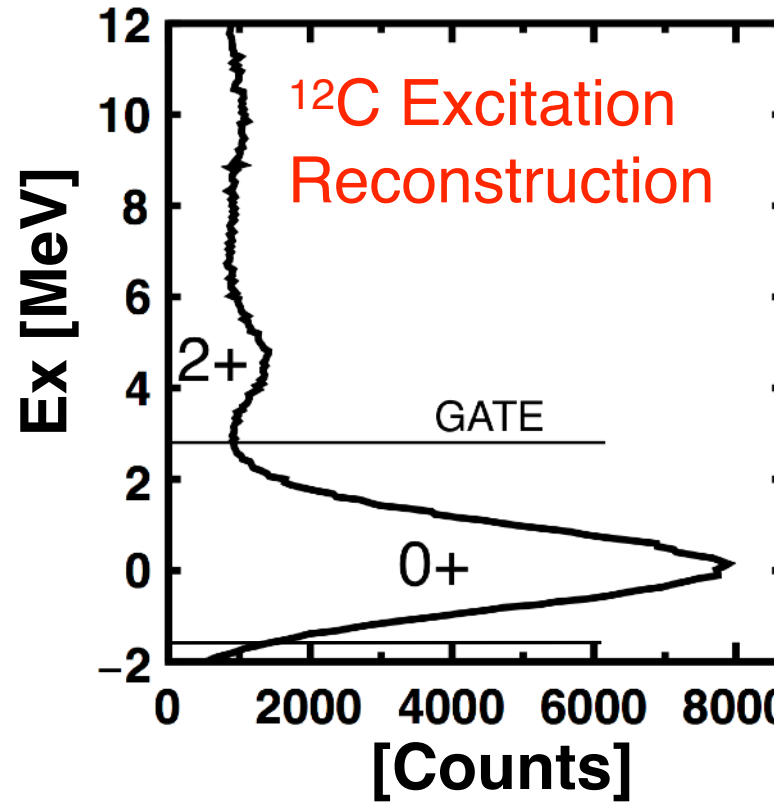
${}^7\text{Li}$ Level Scheme



We reconstruct events by adding momentum back together.



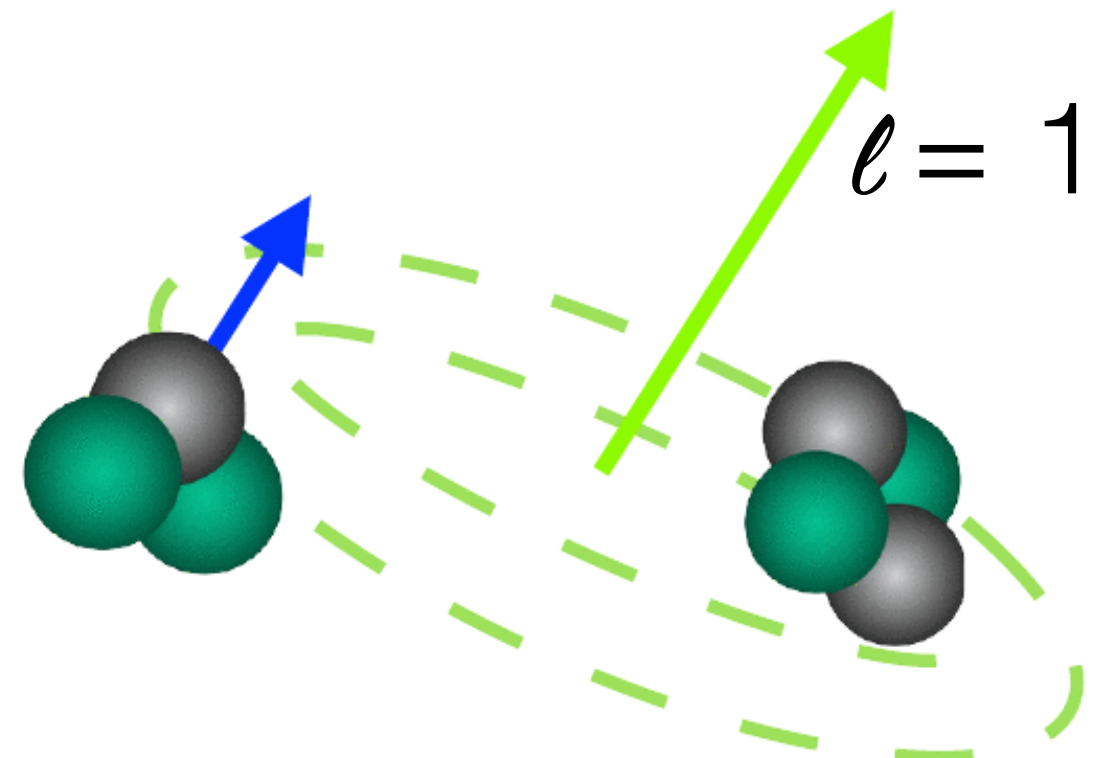
${}^{12}\text{C}$ Level Scheme



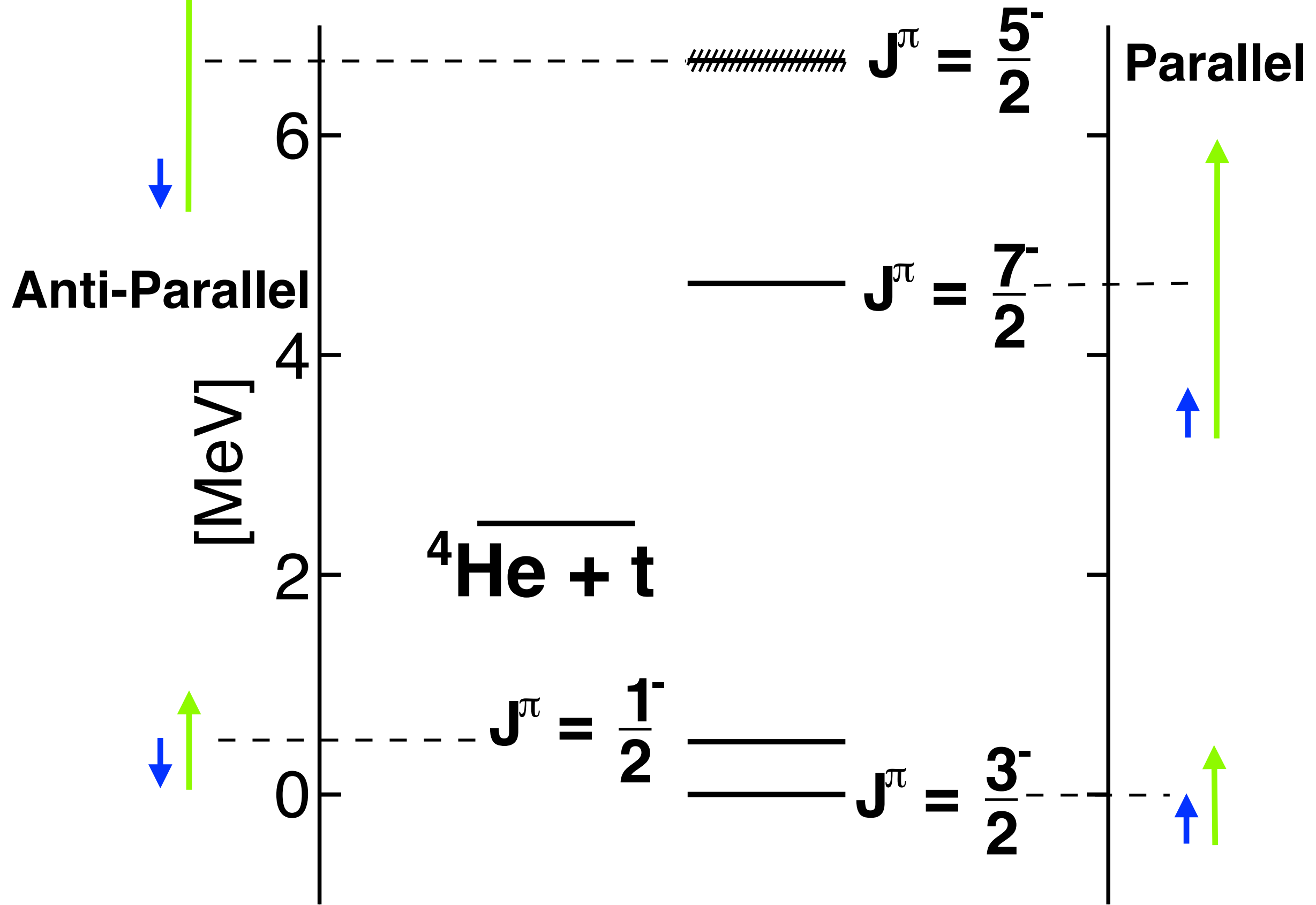
We know 3/4 parts of the Kinematics for
 ${}^7\text{Li} + {}^{12}\text{C} \rightarrow {}^7\text{Li}^* + {}^{12}\text{C}(\text{GS})$
so we can deduce the target's excitation energy as well.

Cluster Model

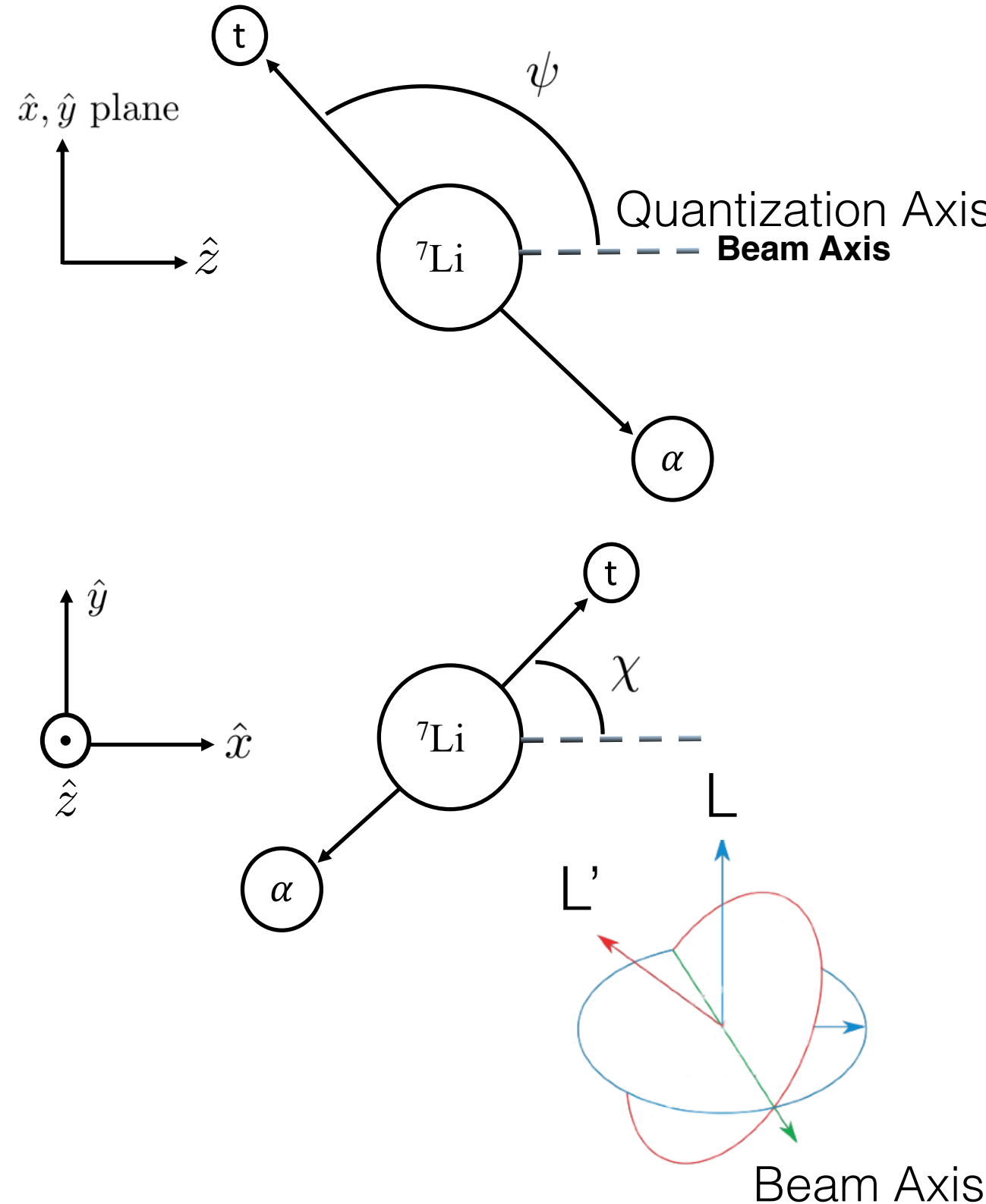
- We treat ${}^7\text{Li}$ as a “cluster” of an α and ${}^3\text{H}$ orbiting each other with angular momentum, ℓ , with projection, μ .
- We describe the g.s. ($J^\pi = 3/2^-$) with $\ell = 1$ and the triton spin parallel to the internal angular momentum.
- The 1st excited state ($J^\pi = 1/2^-$) has $\ell = 1$ with the triton spin anti-parallel.
- The 2nd excited state ($J^\pi = 7/2^-$) has $\ell = 3$ with the triton spin parallel.
- The 3rd excited state ($J^\pi = 5/2^-$) has $\ell = 3$ with the triton spin anti-parallel.



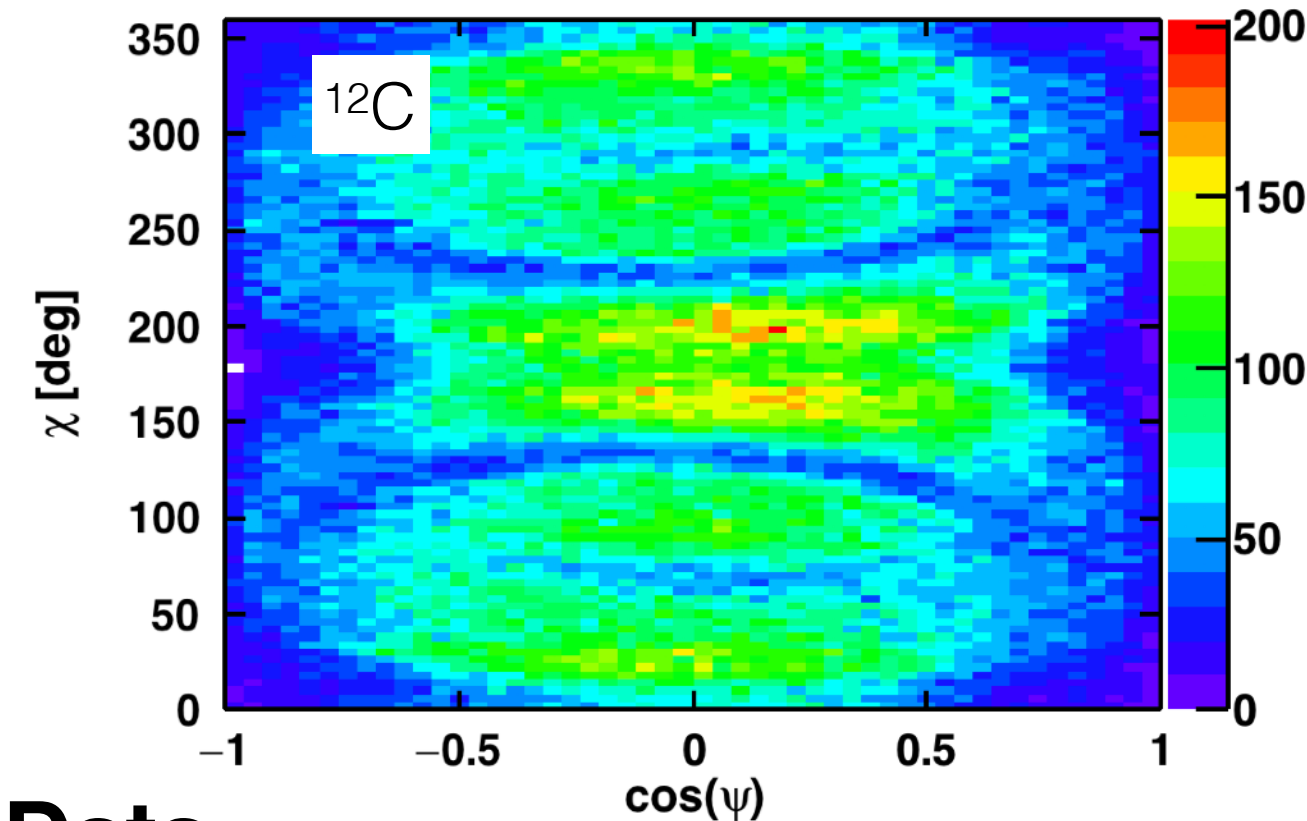
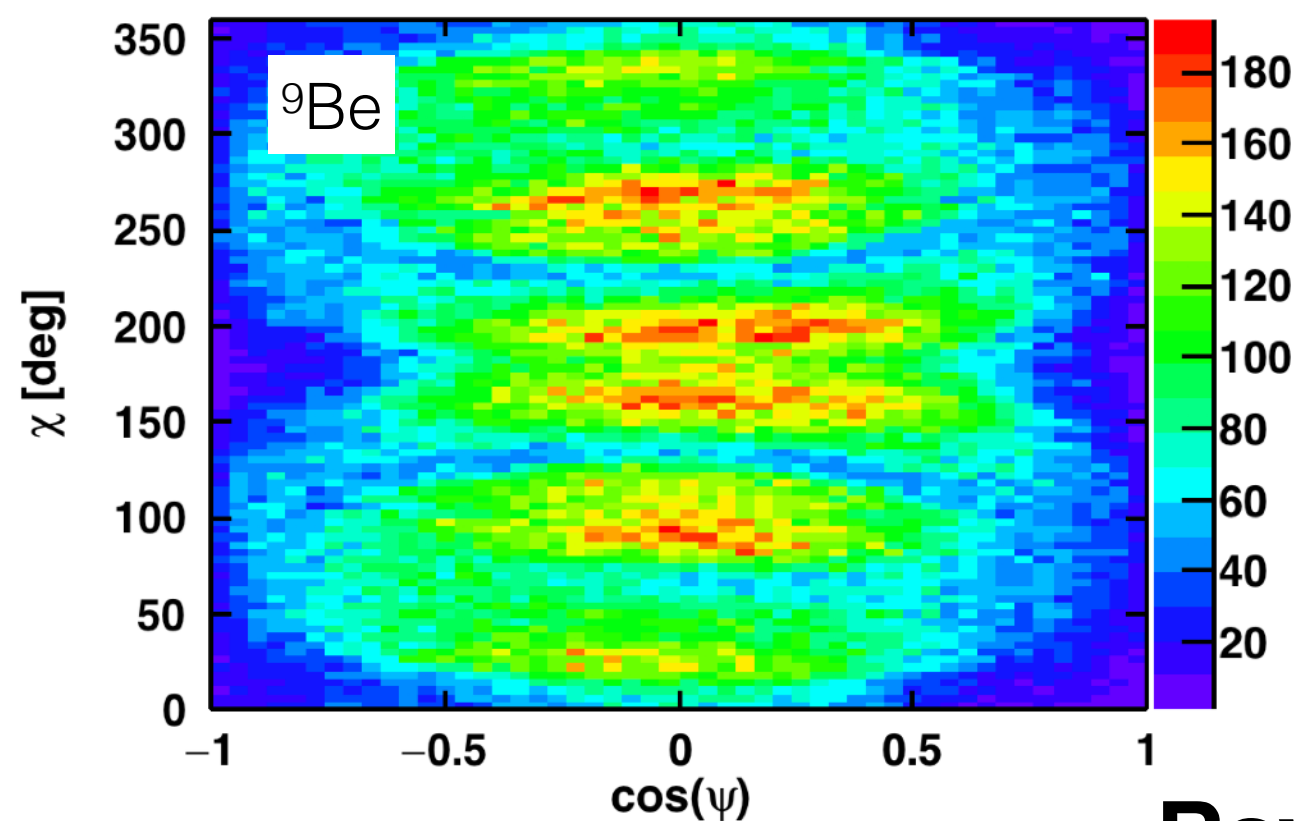
^7Li Level Scheme



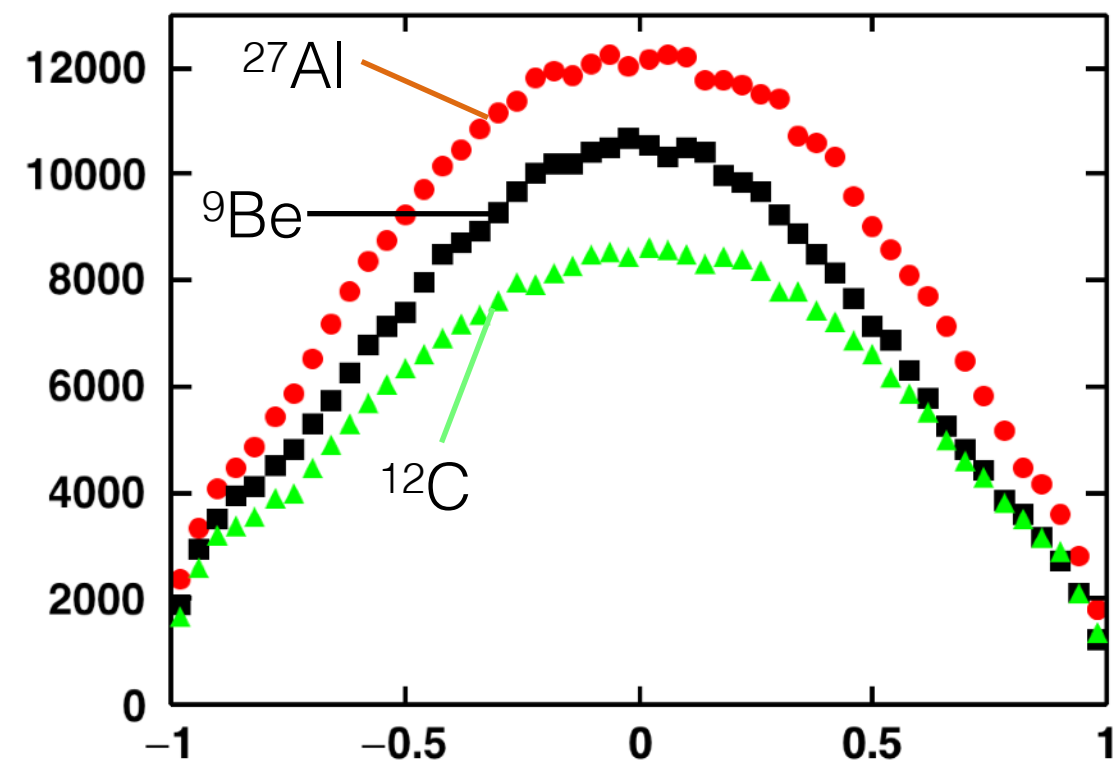
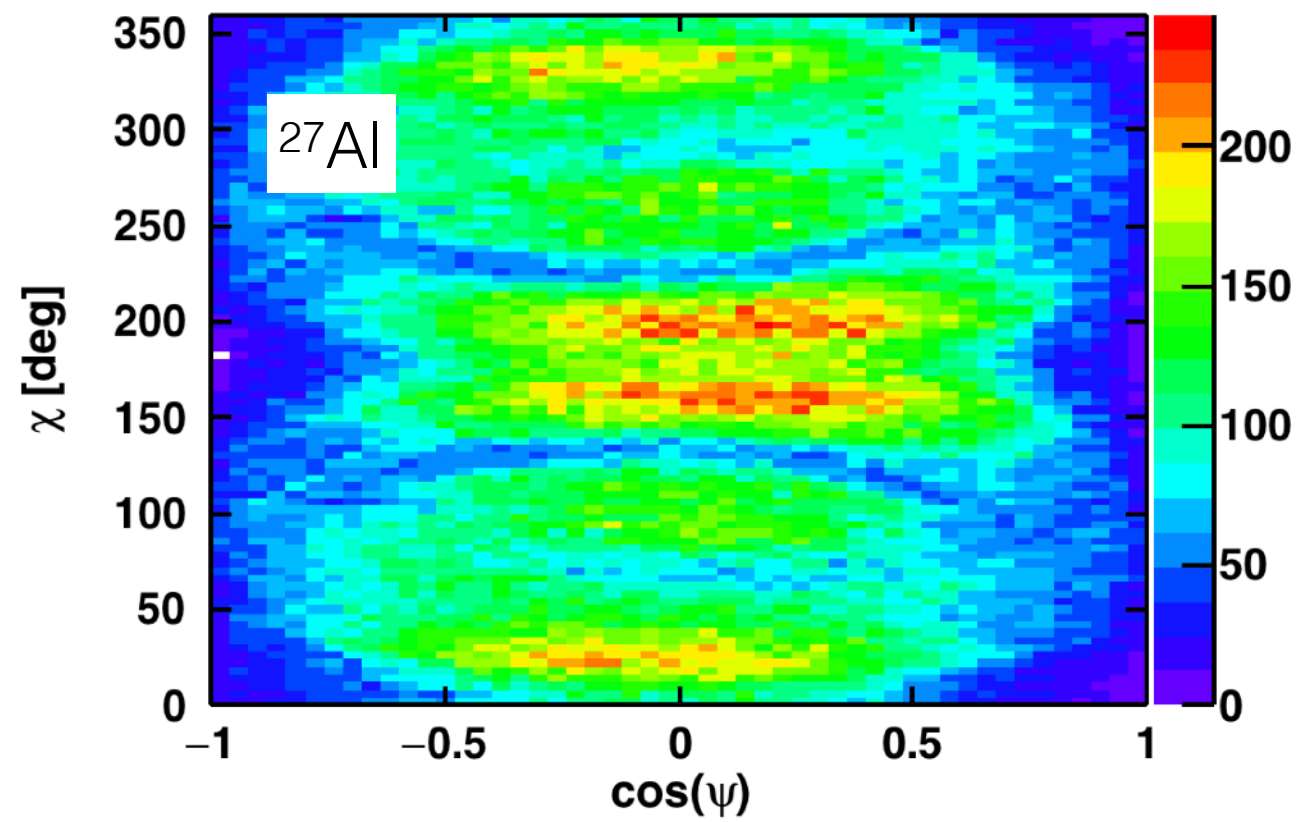
How do we determine spin alignment?

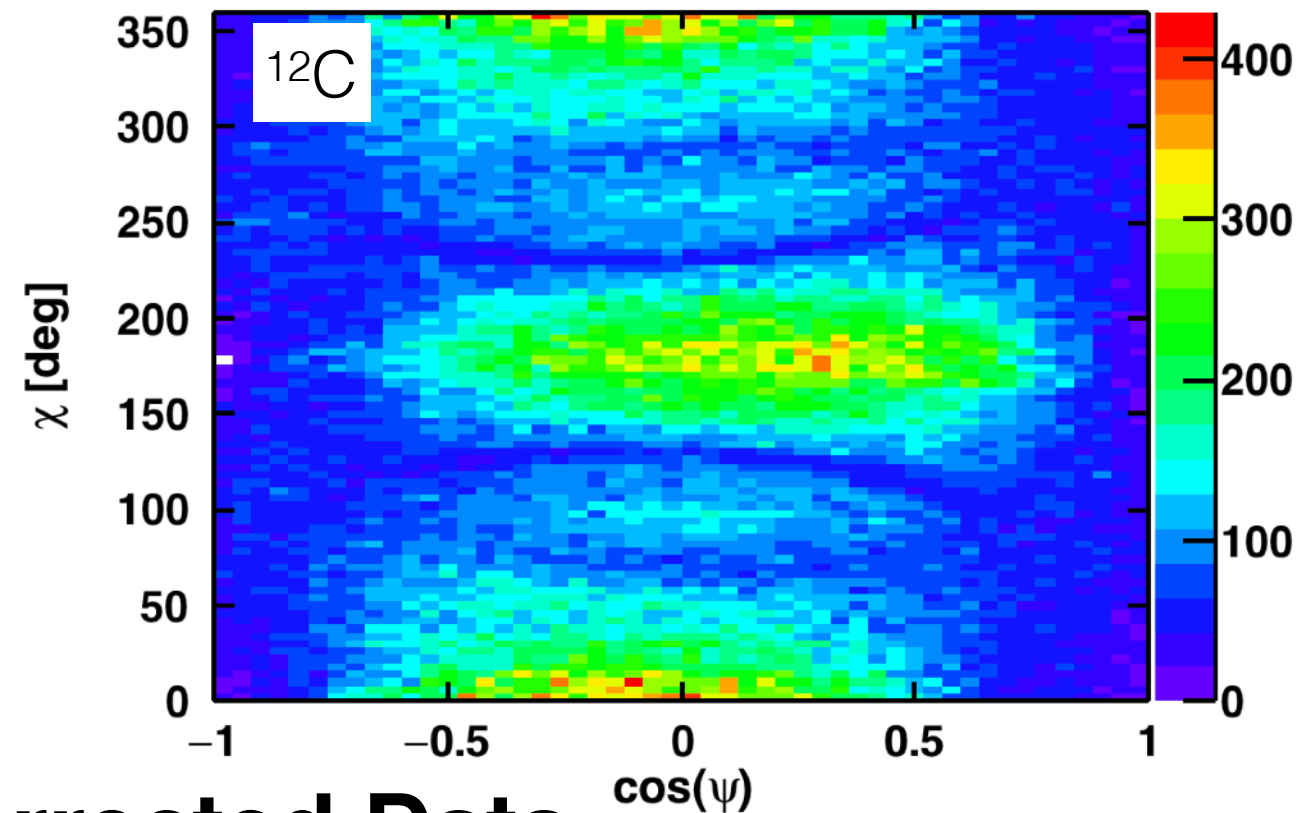
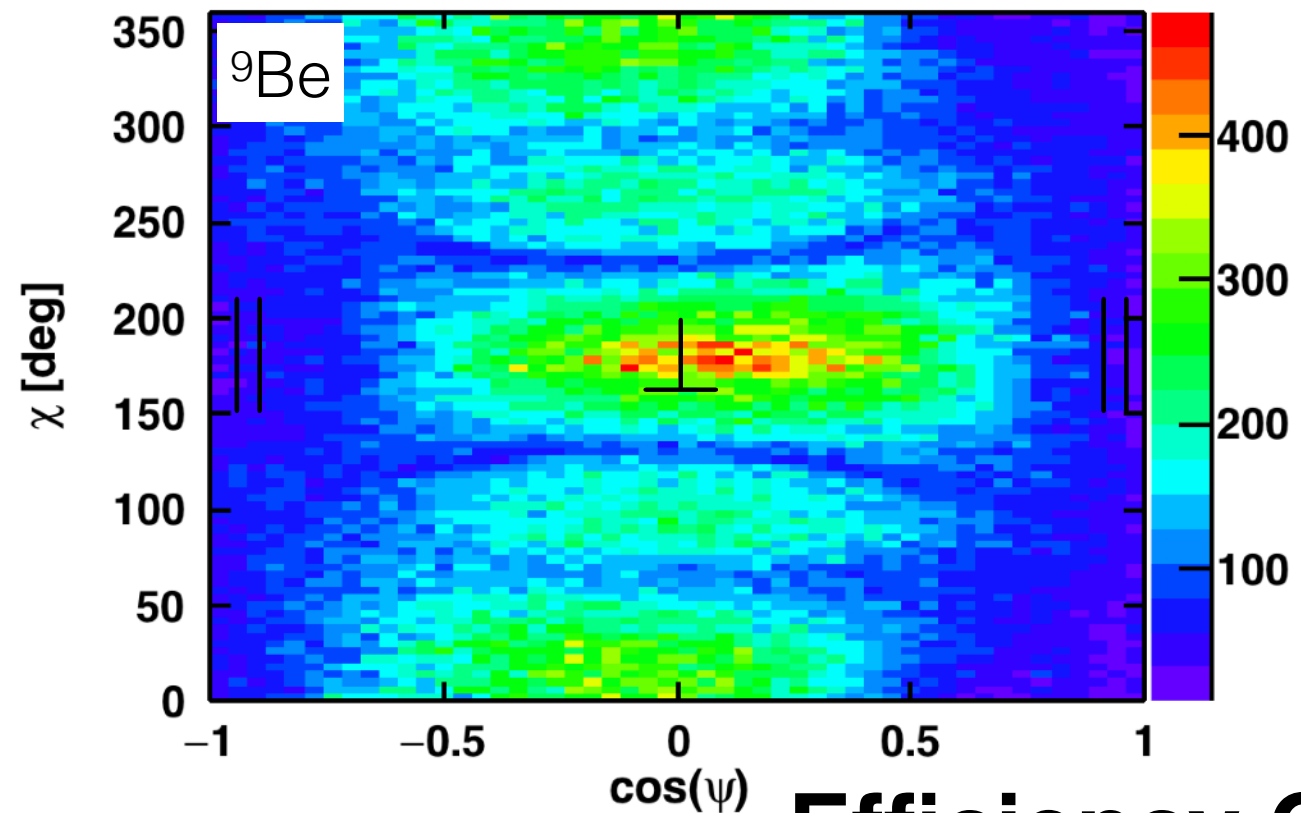


- Decay of $7/2^-$ state has $\ell_{\text{final}} = 3$ ($\alpha+t$ internal A.M.)
- If A.M. is **perpendicular** to the beam-axis fragments of decay will be preferentially emitted in a plane containing the beam axis ($\psi = 0^\circ$).
- If A.M. is **parallel** to the beam-axis fragments of decay will be preferentially emitted in the x-y plane ($\psi = 90^\circ$).

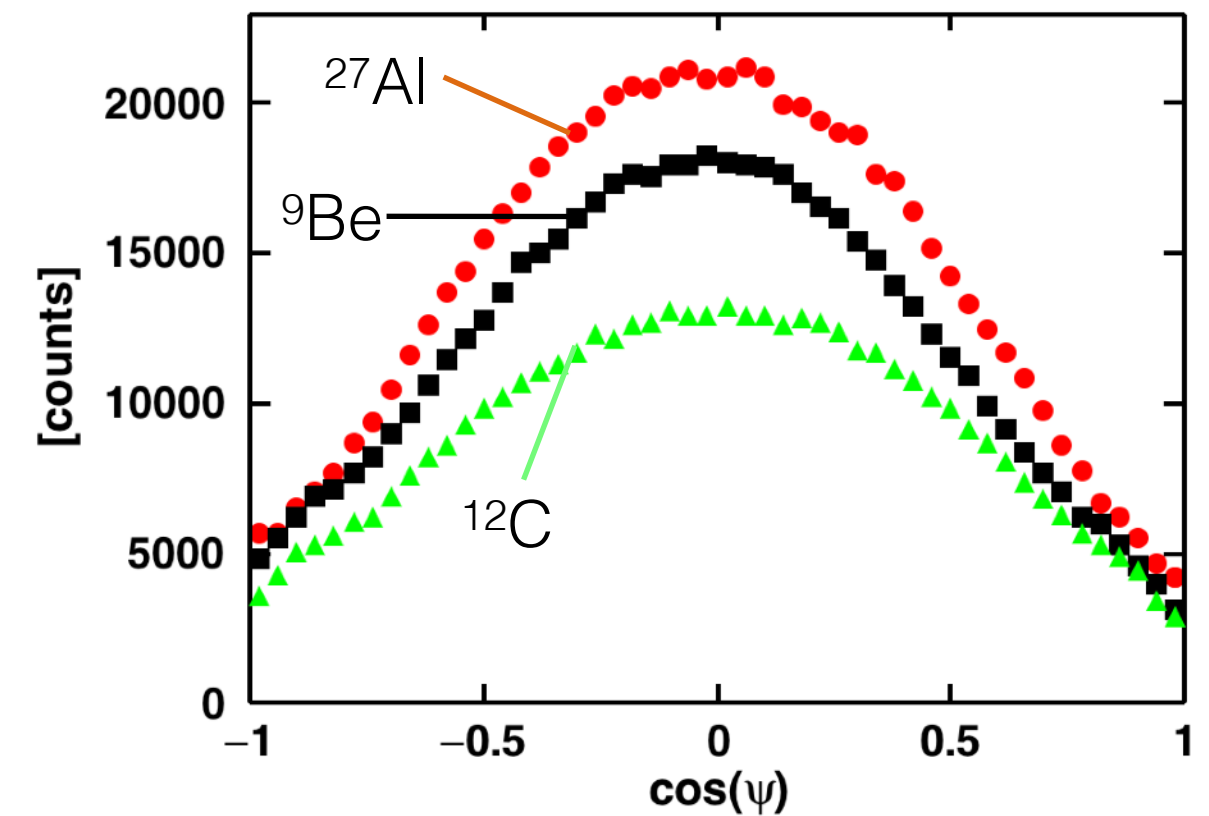
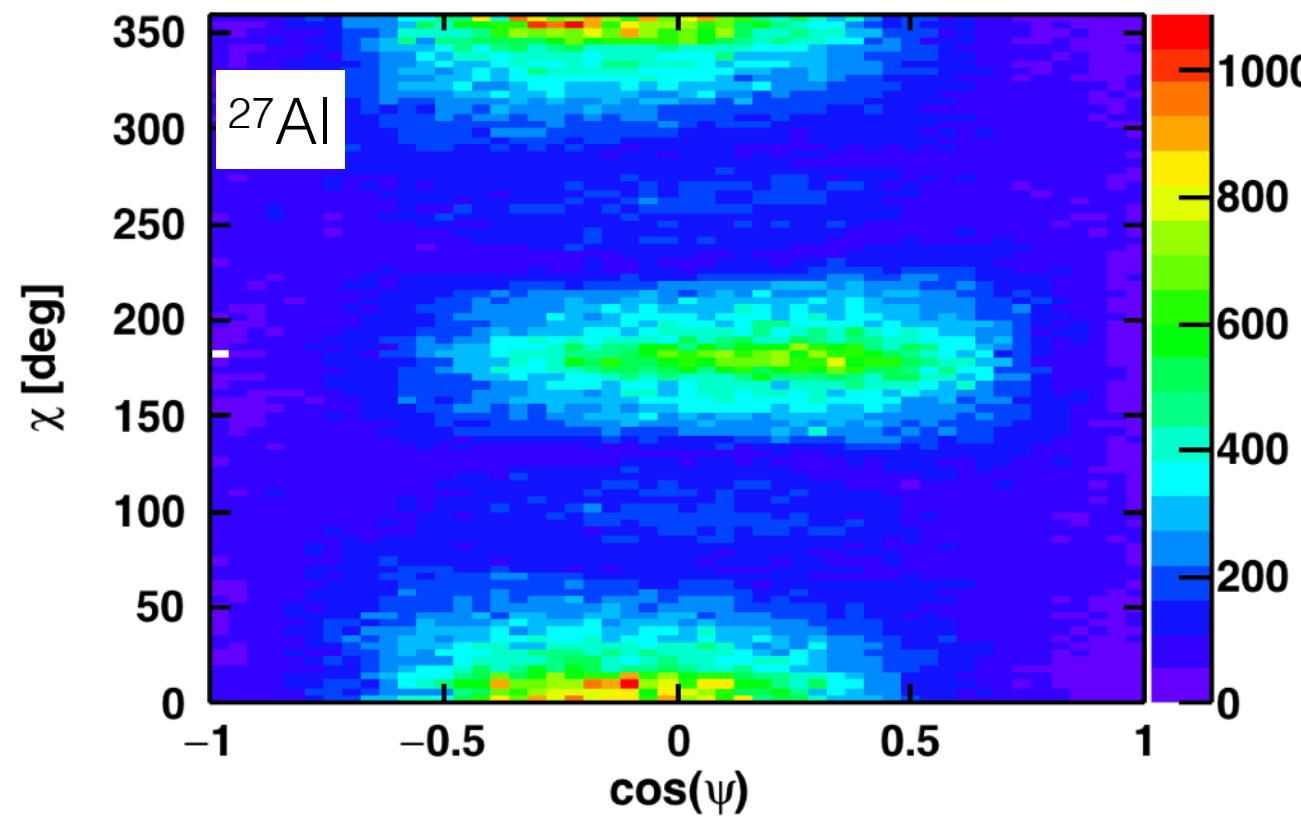


Raw Data





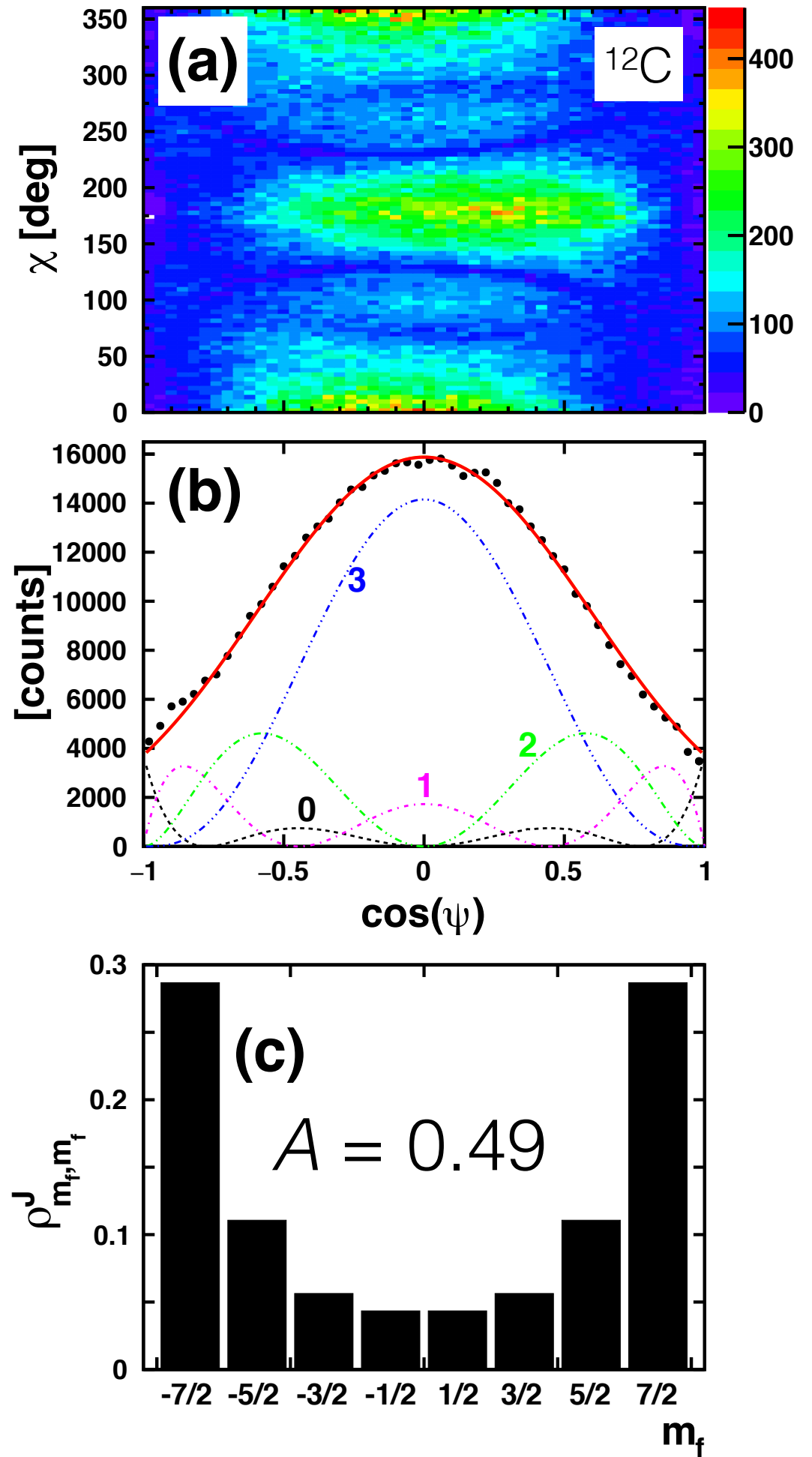
Efficiency Corrected Data



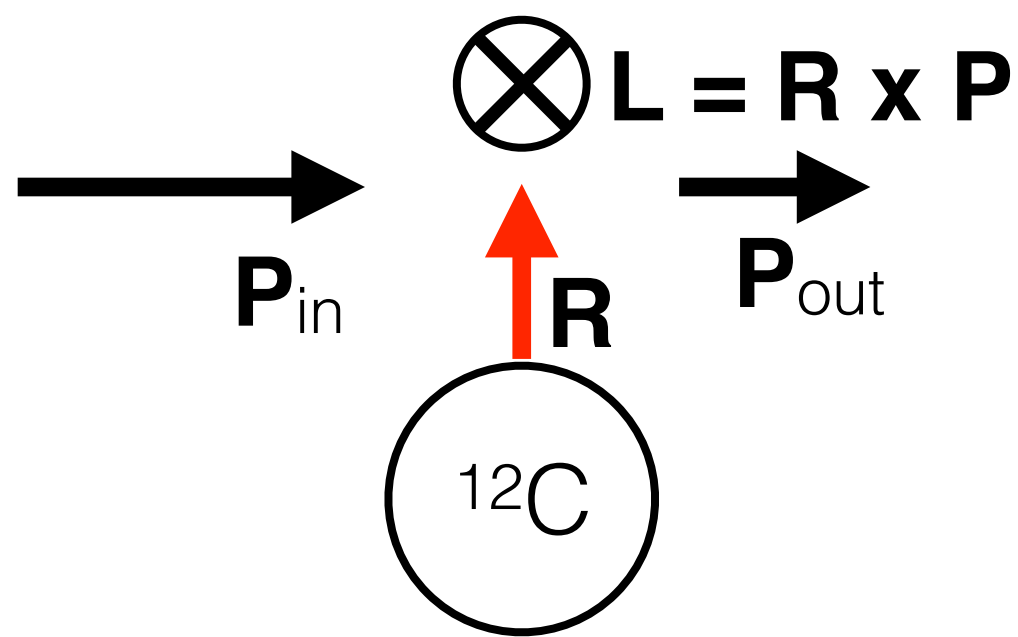
Strong peak at $\cos(\psi) = 0$

Magnetic Substate Extraction

- For the rest of the talk I'll focus on the reaction with ^{12}C .
- We fit the angular correlations to Legendre Polynomials to extract the magnetic sub-state.
- The weights of the Legendre Polynomials are related to the population of the magnetic substate.
- Extracted magnetic sub-states indicate large *longitudinal* alignment.



Angular Momentum & Excitation Energy Matching

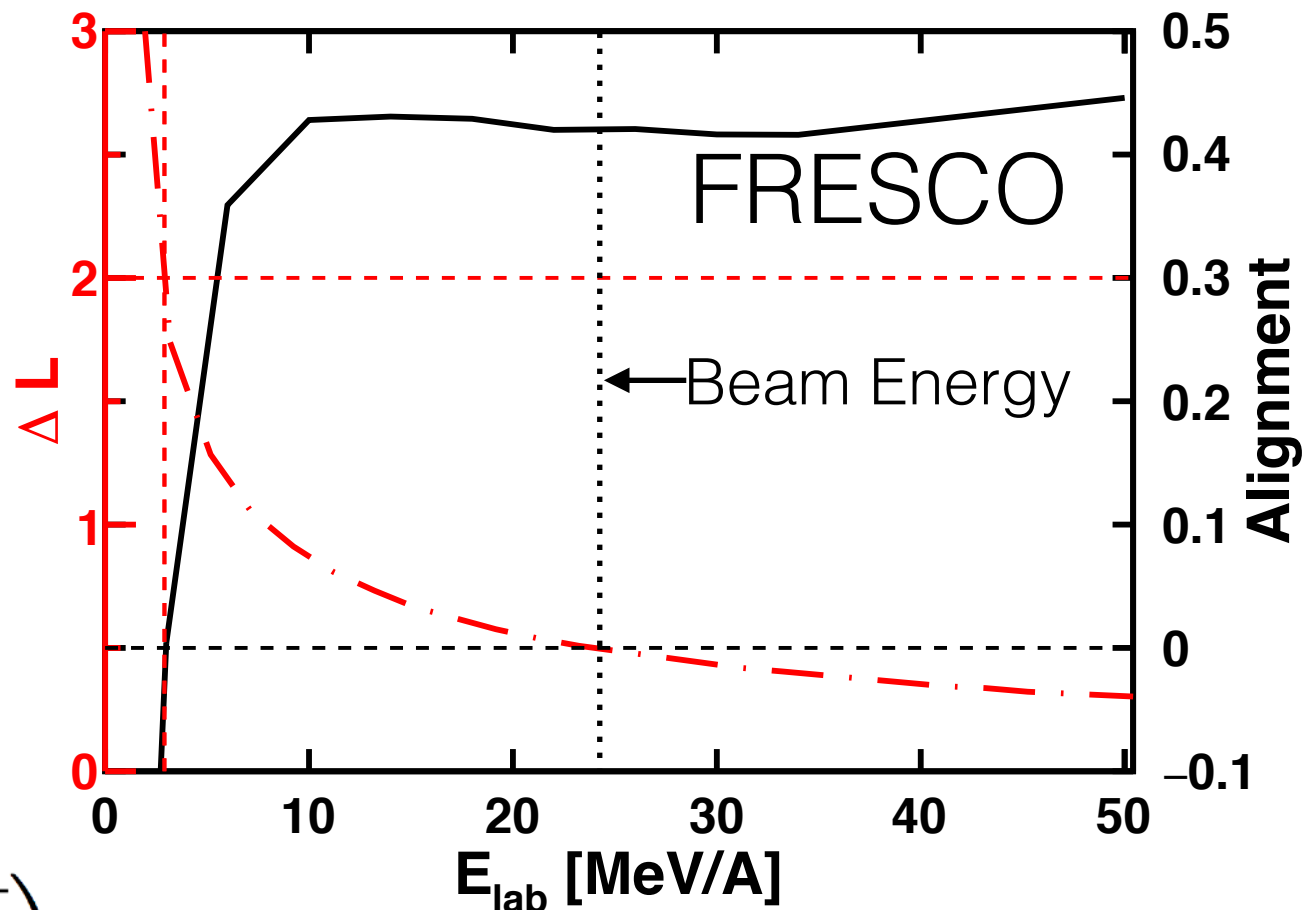


$$\Delta L = \mathbf{R} \times (\mathbf{P}_{in} - \mathbf{P}_{out})$$

$$= R \sqrt{2\mu E_{CM}} \left(1 - \sqrt{1 - \frac{E^*}{E_{CM}}} \right)$$

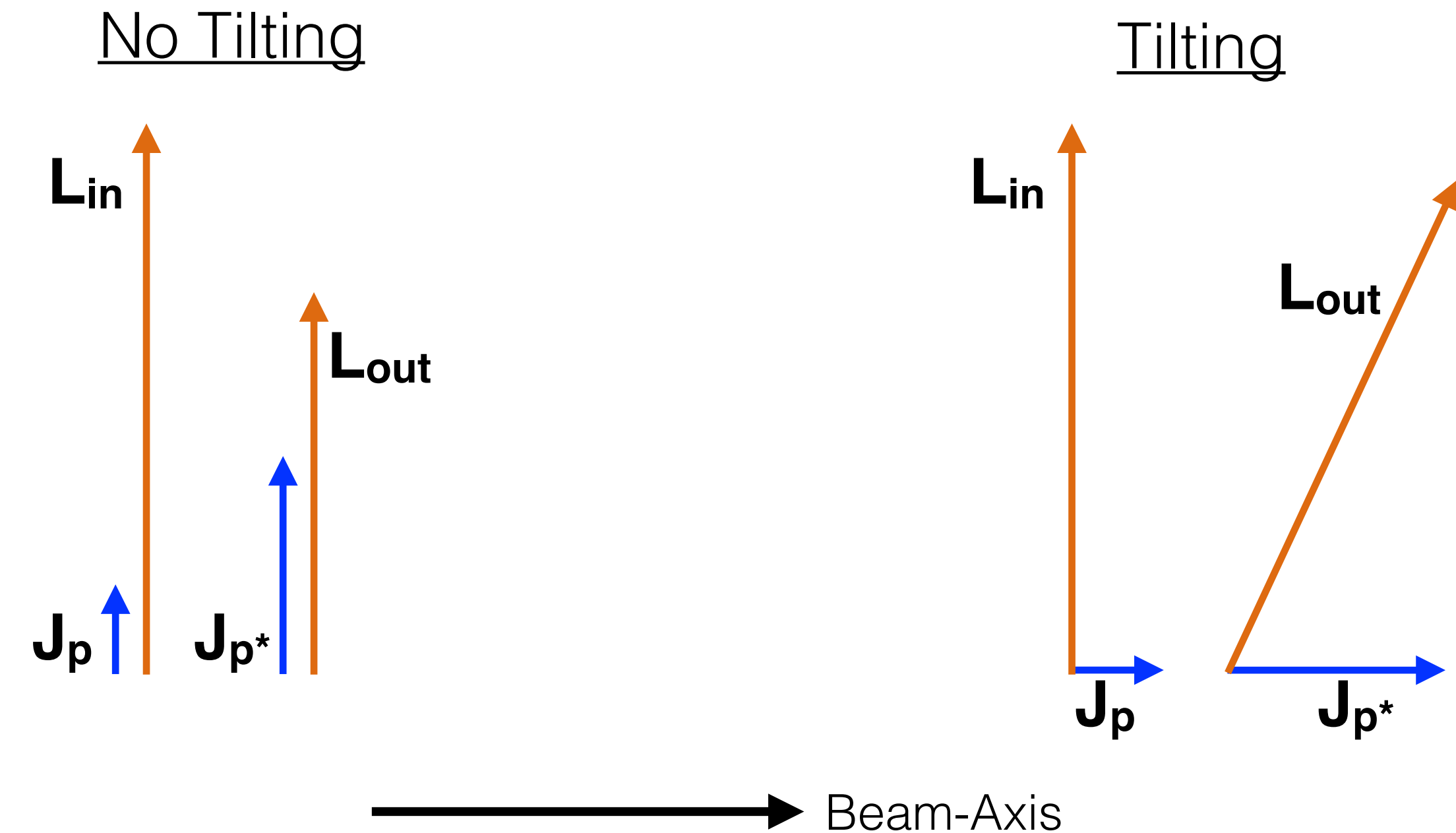
$R \sim 5$ fm, $E^* = 4.68$ MeV

$\Delta\ell = 2$



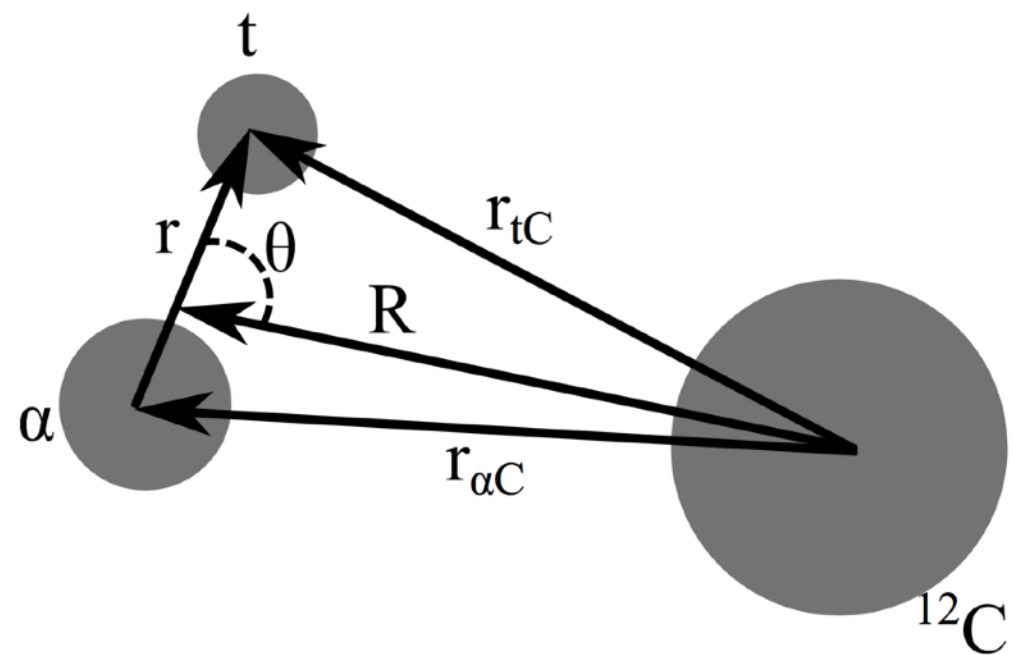
Reaction-plane must **TILT** to conserve A.M. above a certain threshold

Angular Momentum & Excitation Energy Matching



Alignment Mechanism

- We looked at the transfer, or T , matrix of the projectile.
- The squared elements of the T -Matrix give the probability of going from an initial to final state. The projection onto m_f gives a predicted m -state distribution.
- The last two integrations are directly proportional to Clebsch-Gordan Coefficients.



$$\begin{aligned}
 T_{m_i, m_f}^L &\propto \sum_{\mu_i, \mu_f, m_s} \langle \ell_i, \mu_i; 1/2, m_s | J_i, m_i \rangle \\
 &\quad \times \langle \ell_f, \mu_f; 1/2, m_s | J_f, m_f \rangle \\
 \text{Internal} \rightarrow &\times \int Y_{-\mu_f}^{\ell_f}(\hat{r}) Y_M^K(\hat{r}) Y_{\mu_i}^{\ell_i}(\hat{r}) d\Omega_r \\
 \text{External} \rightarrow &\times \int Y_{-M}^L(\hat{R}) Y_M^K(\hat{R}) Y_0^L(\hat{R}) d\Omega_R, \\
 \text{A.M. \& E* matching} \rightarrow & L_{\text{in}} = L_{\text{out}}
 \end{aligned}$$

$$\mathbf{J} = \ell + 1/2$$

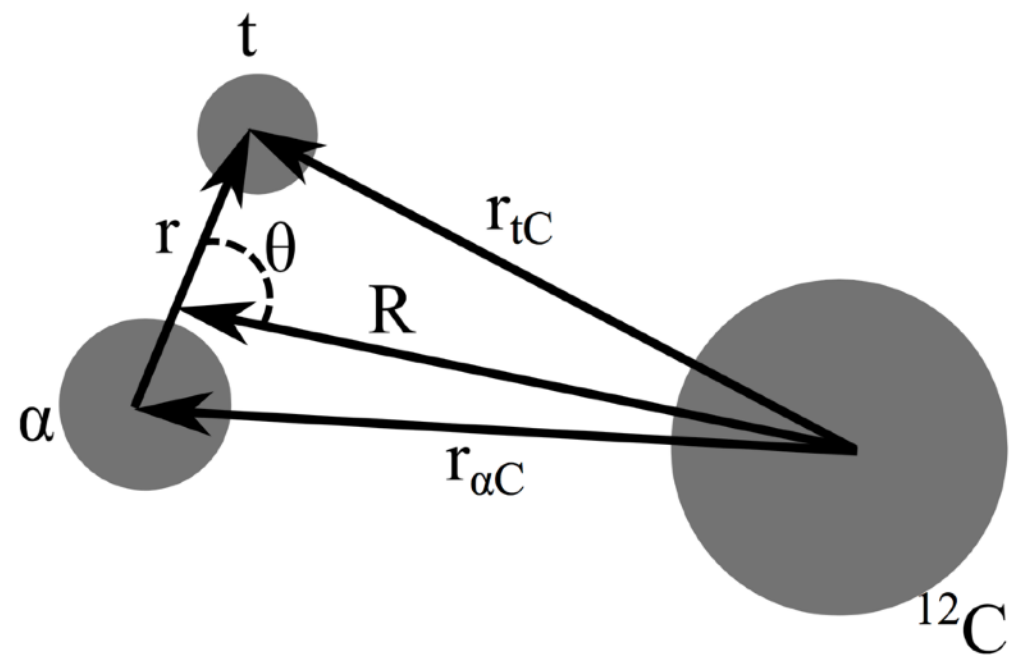
$$\ell_i = 1 \rightarrow J_i = 3/2 \quad \ell_f = 3 \rightarrow J_f = 7/2$$

$$M = \Delta\mu = \Delta m = m_f - m_i$$

$$K = 2 \text{ (from parity)}$$

Alignment Mechanism

- We looked at the transfer, or T , matrix of the projectile.
- The squared elements of the T -Matrix give the probability of going from an initial to final state. The projection onto m_f gives a predicted m -state distribution.
- The last two integrations are directly proportional to Clebsch-Gordan Coefficients.



$$T_{m_i, m_f}^L \propto \langle J_i, m_i ; K, M | J_f, m_f \rangle \\ \times \langle L, 0 ; K, M | L, M \rangle .$$

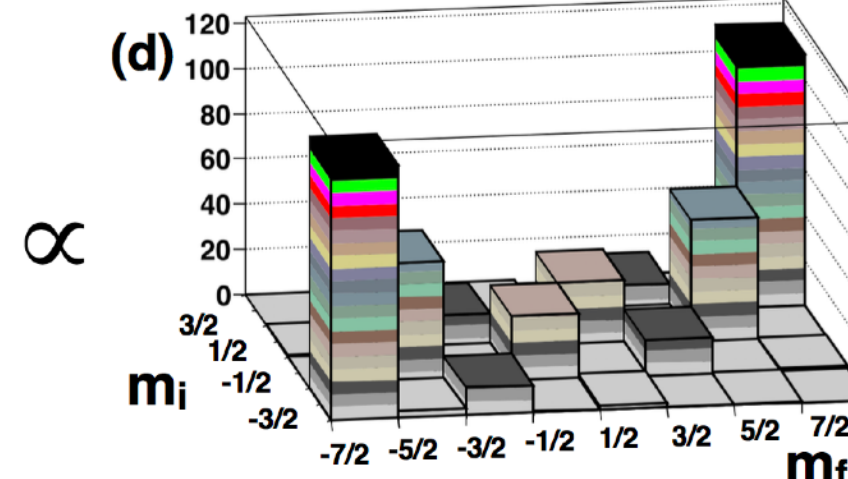
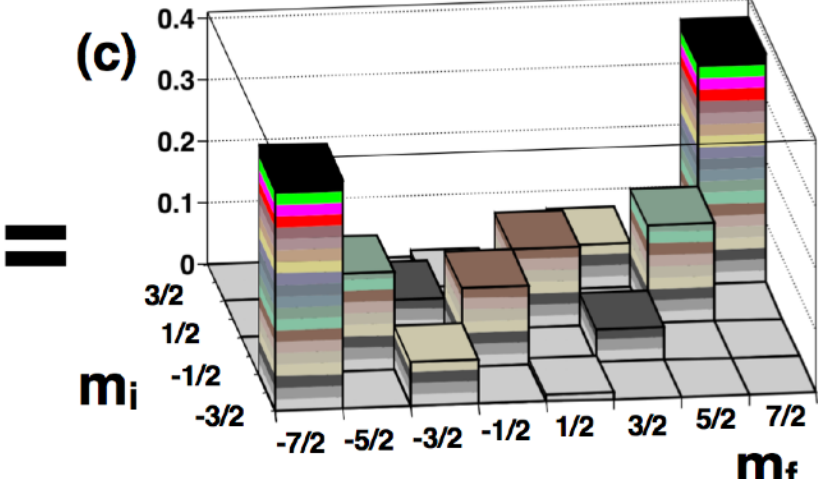
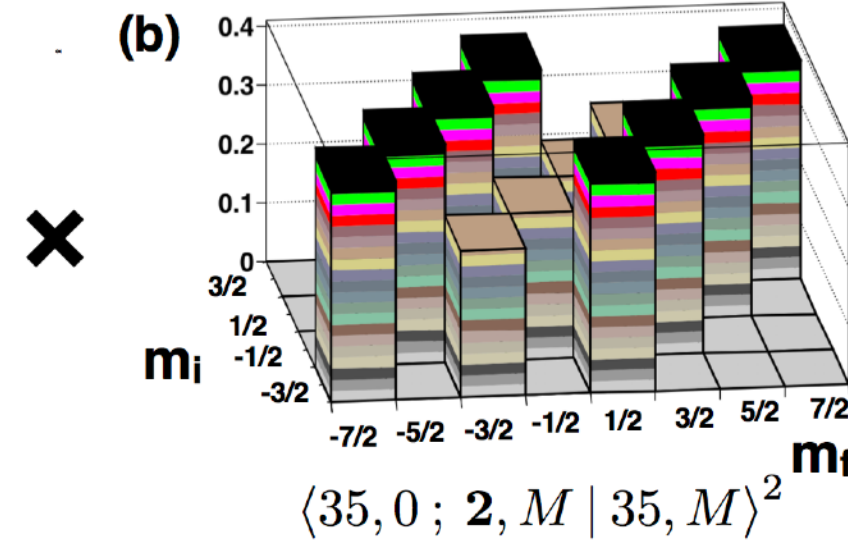
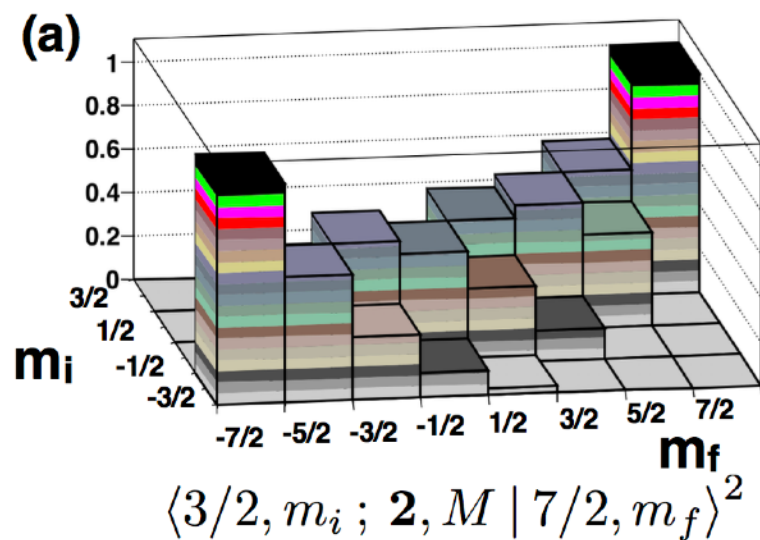
$$\mathbf{J} = \ell + 1/2$$

$$\ell_i = 1 \rightarrow J_i = 3/2 \quad \ell_f = 3 \rightarrow J_f = 7/2$$

$$M = \Delta\mu = \Delta m = m_f - m_i$$

$$K = 2 \text{ (from parity)}$$

Alignment Mechanism

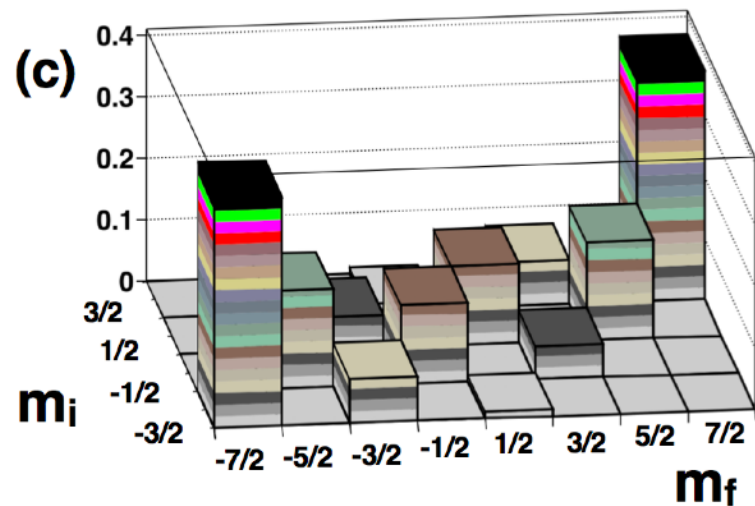


$M = \pm 1$ is completely suppressed

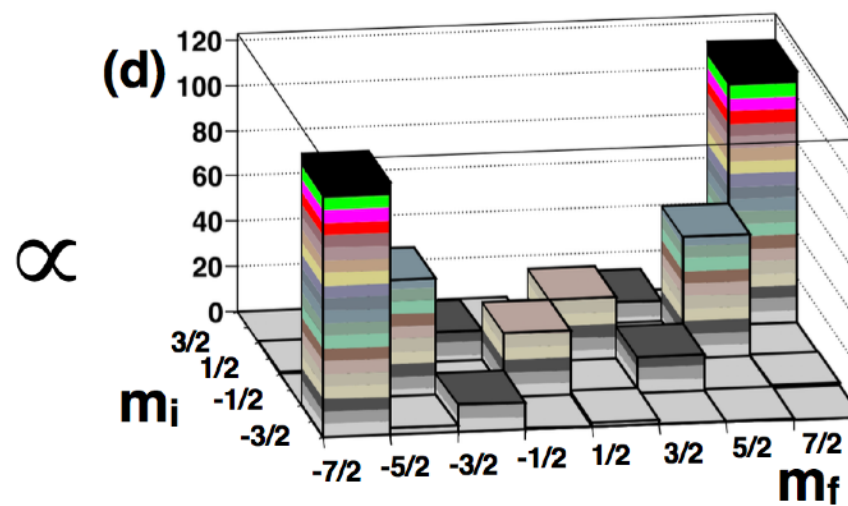
Multiplying together the relevant Clebsch-Gordan coefficients predicts a squared T-Matrix.

The squared T-Matrix from FRESCO is strikingly similar to the CG prescription.

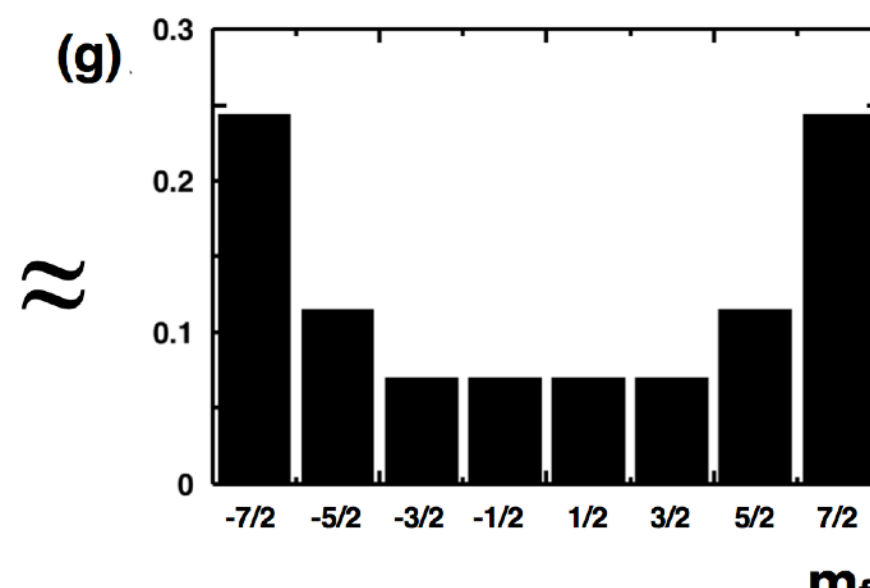
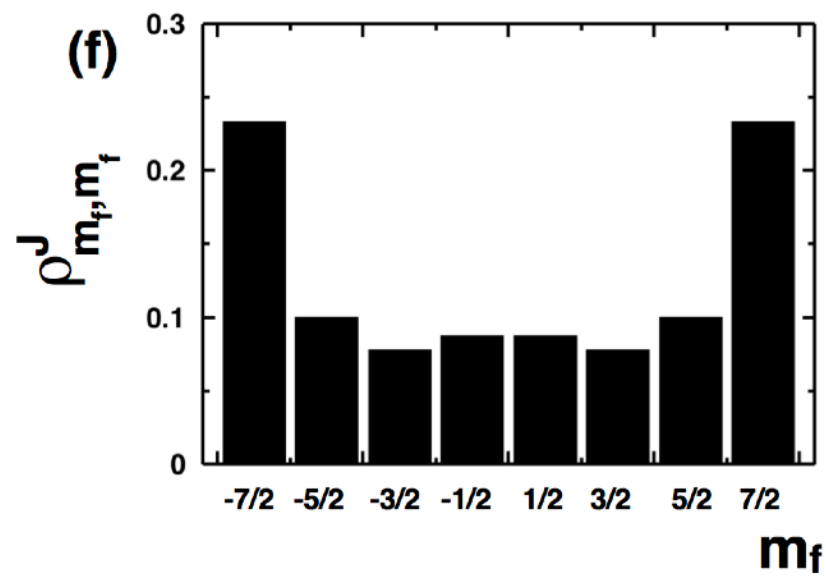
Alignment Mechanism



$$\langle 3/2, m_i ; \mathbf{2}, M | 7/2, m_f \rangle^2 \langle 35, 0 ; \mathbf{2}, M | 35, M \rangle^2$$



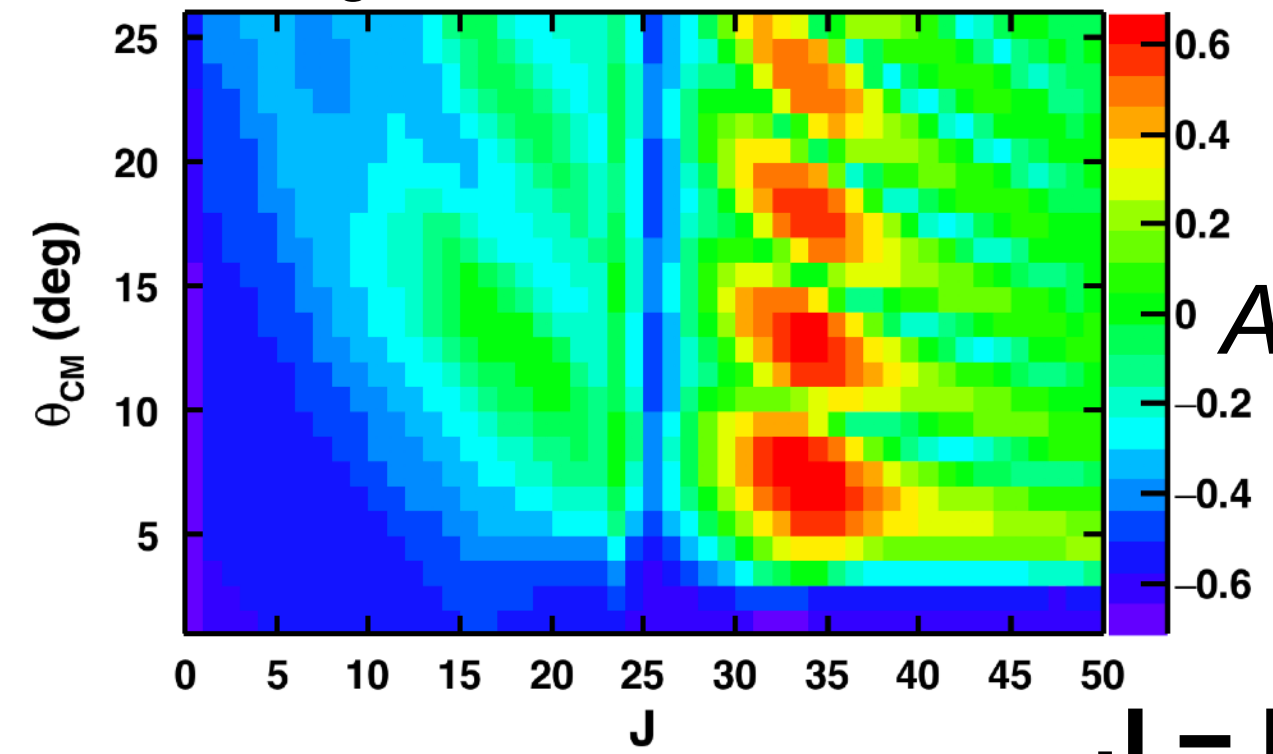
Multiplying together the relevant Clebsch-Gordan coefficients predicts a squared T-Matrix.



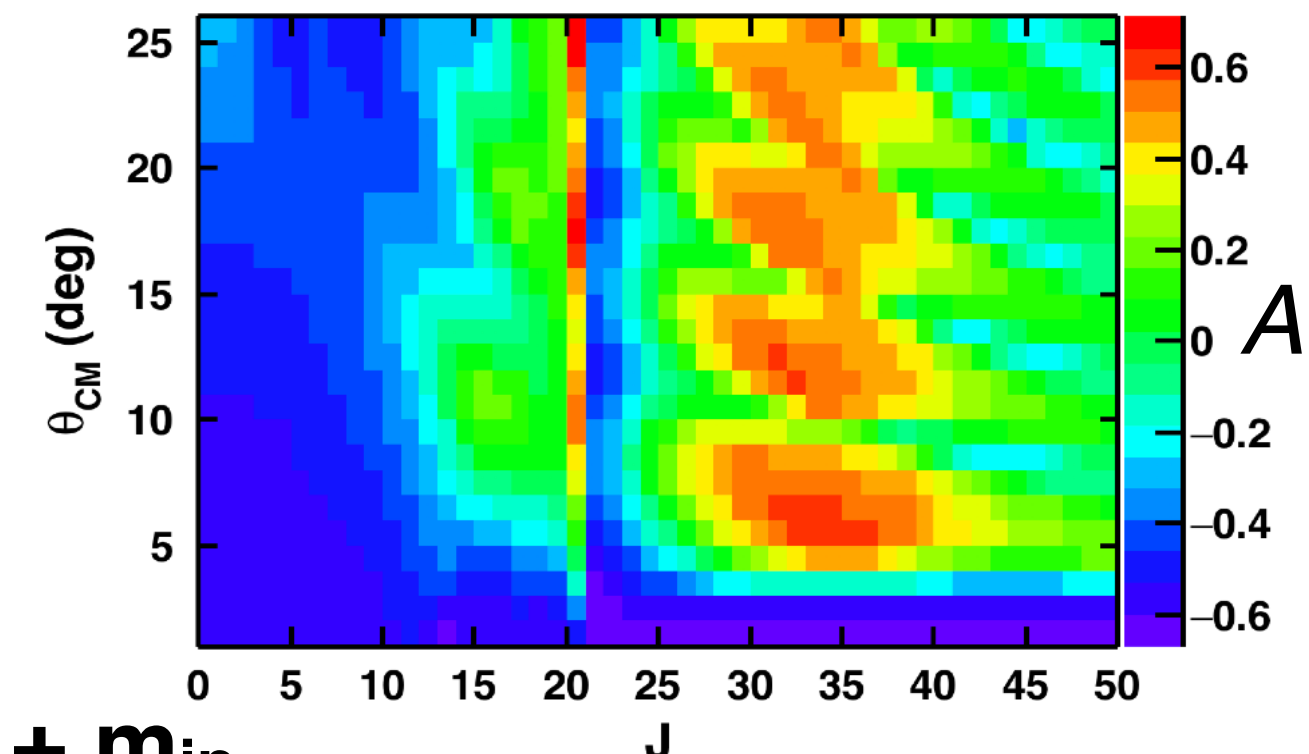
The squared T-Matrix from FRESCO is strikingly similar to the CG prescription.

L-Wave Mixing → Alignment

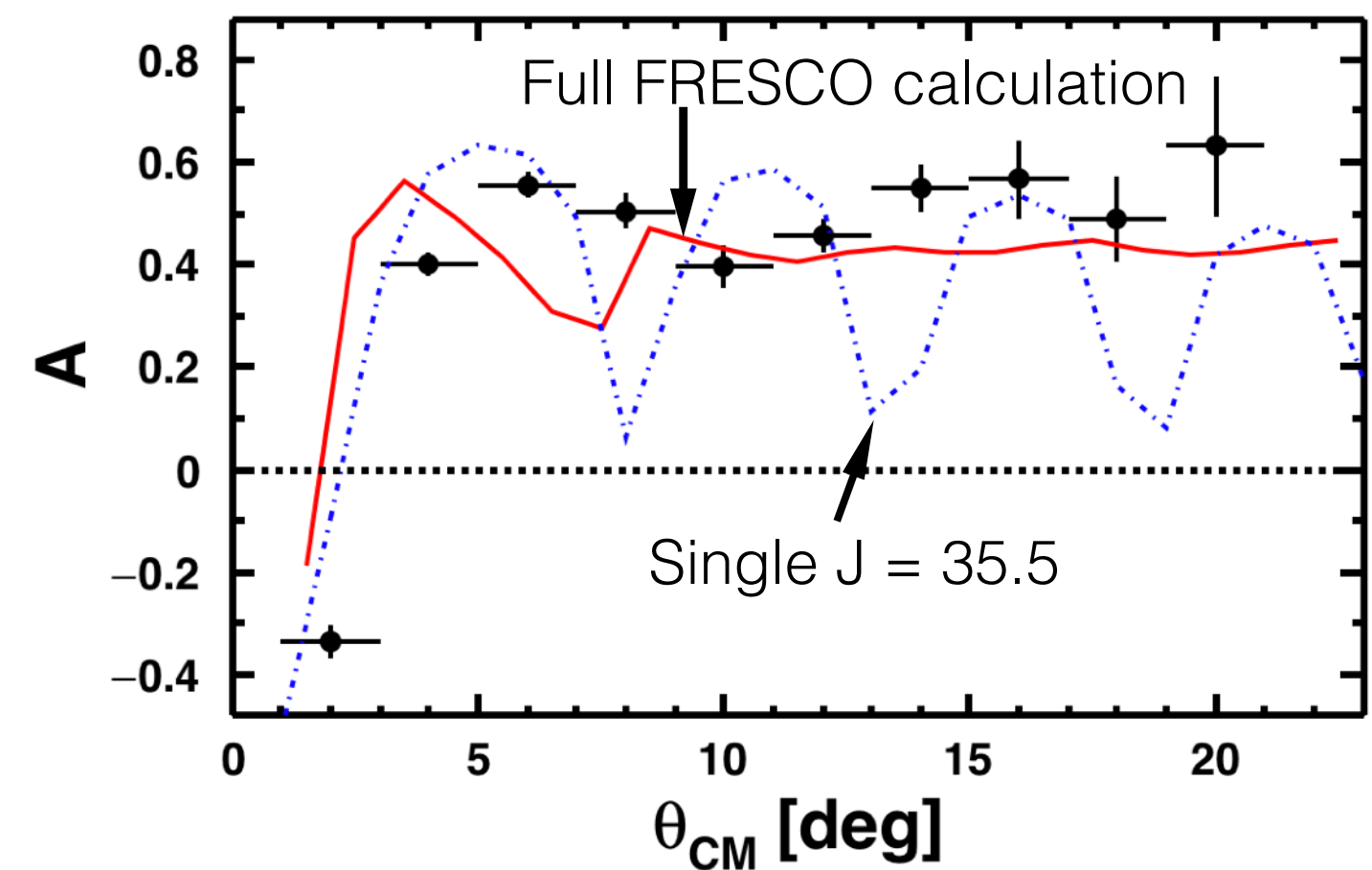
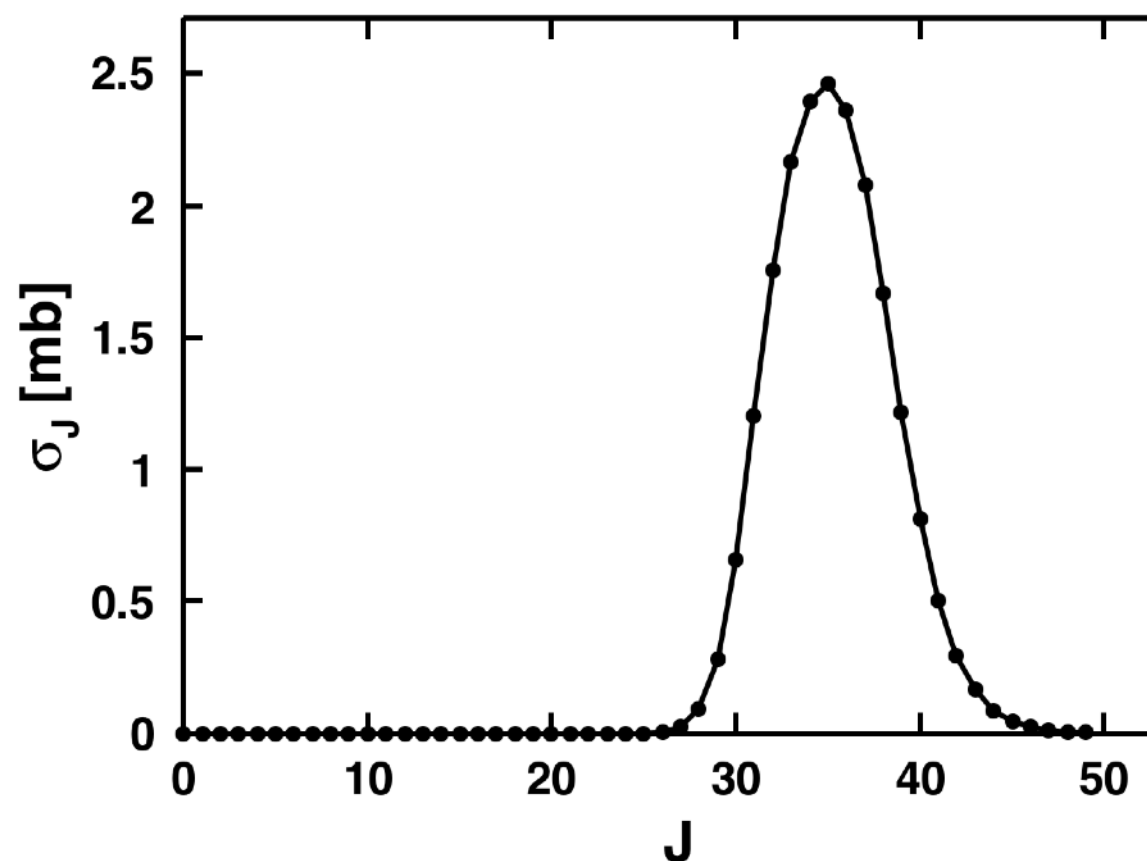
Single J FRESCO calculations



± 4 J FRESCO calculations



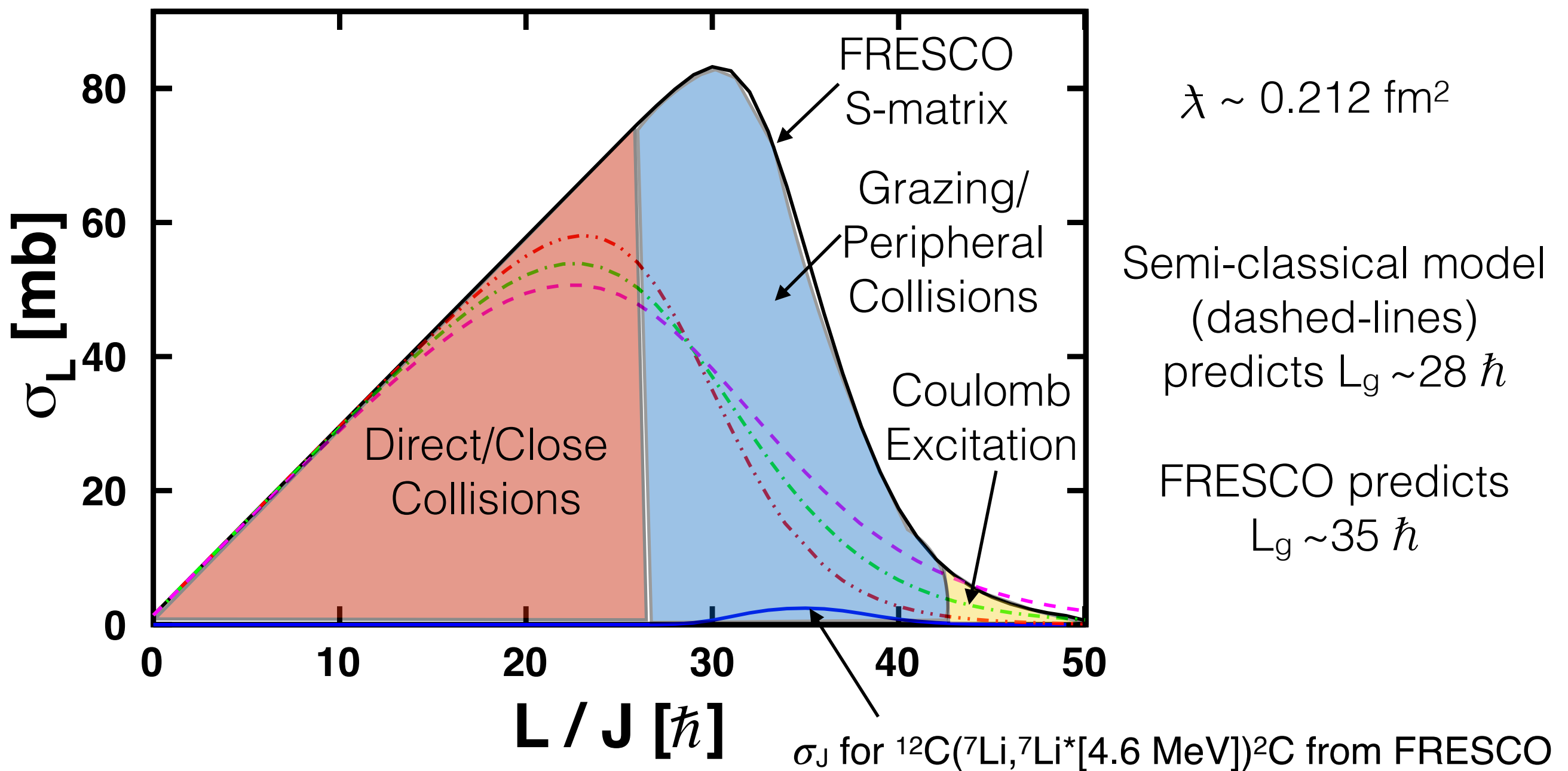
$$J = L + m_{\text{in}}$$



Characterizing the Reaction

${}^7\text{Li} + {}^{12}\text{C}$ with 24 MeV/A ${}^7\text{Li}$

$$\sigma_R = \pi \lambda^2 \sum_{L=0}^{\infty} (2L+1)(1 - |\mathbf{S}_L|^2)$$



Conclusions

- Uncovered alignment mechanism that was buried in standard scattering theory.
- Alignment arises from an angular-momentum-excitation-energy mismatch.
- Many L-waves interfere resulting in the alignment being a smooth function of scattering angle for large angles.
- Alignment mechanism is independent of the scattering potential used.
 - Could be found in many scattering experiments.

Partial-Wave Analysis

Separate variables in the Hamiltonian and focus on radial part,

$$\left[\frac{-\hbar^2}{2m} \frac{d^2}{dr^2} + \frac{\hbar^2 L(L+1)}{2mr^2} + V(\mathbf{r}) \right] \psi(\mathbf{r}) = E\psi(\mathbf{r})$$

Using the Bohr approximation we treat the incoming particle as a plane-wave,

$$\psi_{\mathbf{k}_{in}}(\mathbf{r}) = e^{-ikz}$$

We can then do a plane-wave expansion giving us,

$$\psi_{\mathbf{k}_{in}}(\mathbf{r}) = e^{-ikz} = \sum_{L=0}^{\infty} (2L+1) i^L j_L(kr) P_L(\cos \theta)$$

Where, $j_L(kr)$, is a spherical Bessel function.

Partial-Wave Analysis

Now we make the ansatz for the full outgoing wavefunction,

$$\psi_{\mathbf{k}_{out}}(\mathbf{r}) = e^{-ikz} + f_k(\theta) \frac{e^{-ikr}}{r}$$

Where, $f_k(\theta)$, is called the “scattering amplitude”. The differential cross section is related to the scattering amplitude by,

$$\frac{d\sigma}{d\Omega} = |f_k(\theta)|^2$$

And with some algebra we have,

$$f_k(\theta) = \frac{1}{k} \sum_{L=0}^{\infty} (2L+1) e^{i\delta_L} \sin(\delta_L) P_L(\cos \theta)$$

where δ_L is called the “phase-shift” and is dependent on the scattering potential used (draw diagram).